How to cite: *Angew. Chem. Int. Ed.* **2023**, *62*, e202311138
doi.org/10.1002/anie.202311138

Water Purification

MXene-based Membranes for Drinking Water Production

Lingzhi Huang, Li Ding, Jürgen Caro,* and Haihui Wang**

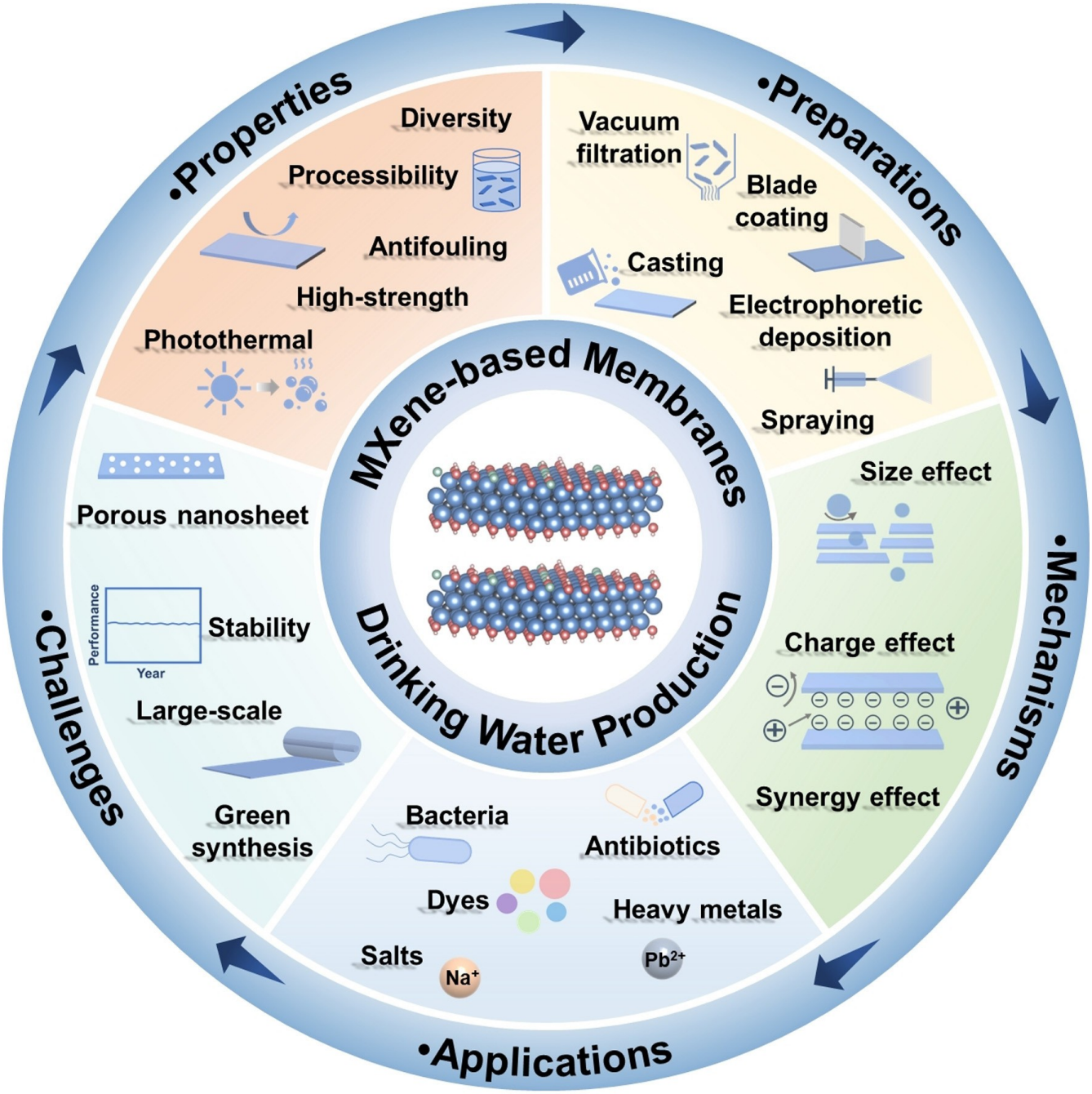

Abstract: The soaring development of industry exacerbates the shortage of fresh water, making drinking water production an urgent demand. Membrane techniques feature the merits of high efficiency, low energy consumption, and easy operation, deemed as the most potential technology to purify water. Recently, a new type of two-dimensional materials, MXenes as the transition metal carbides or nitrides in the shape of nanosheets, have attracted enormous interest in water purification due to their extraordinary properties such as adjustable hydrophilicity, easy processibility, antifouling resistance, mechanical strength, and light-to-heat transformation capability. In pioneering studies, MXene-based membranes have been evaluated in the past decade for drinking water production including the separation of bacteria, dyes, salts, and heavy metals. This review focuses on the recent advancement of MXene-based membranes for drinking water production. A brief introduction of MXenes is given first, followed by descriptions of their unique properties. Then, the preparation methods of MXene membranes are summarized. The various applications of MXene membranes in water treatment and the corresponding separation mechanisms are discussed in detail. Finally, the challenges and prospects of MXene membranes are presented with the hope to provide insightful guidance on the future design and fabrication of high-performance MXene membranes.

1. Introduction

With the rapid population growth, urbanization, industrialization, and escalating agriculture, the freshwater shortage is becoming severer.[1] Therefore, providing clean and drinkable water has been an urgent concern for human living worldwide.[2] Purifying wastewater, brackish water, or seawater can effectively supply sufficient water sources.[3] The efficient simultaneous removal of various impurities such as bacteria and viruses, hormones and pharmaceuticals, dyes, heavy metals, and further organic and inorganic pollutants is still a challenge.[4] Therefore, searching for a highly efficient water purification technology is vital to solving this problem. Membrane techniques have been widely applied in water treatment because they combine high efficiency, low energy consumption, easy operation, and continuous processing.[5] Recently, the booming of two-dimensional (2D) materials further accelerated the development of membrane techniques and opened a new era of advanced membranes.[6] The 2D materials with nanosheets of atomic thickness can be easily modified, thus enabling the ultrafine engineering of membrane structures to fabricate high-performance membranes.[7]

MXenes, a new family of 2D materials, were first synthesized in 2011, known as nanosheets of transition metal carbides or nitrides.[8] Naguib et al.[8] successfully prepared the first MXene nanosheets in an etching process from the parent MAX phase, which are typically composed of layered ternary carbides and nitrides.[9] In general, the MAX phase has the formula of $M_{n+1}AX_n$, where M represents an early transition metal, A represents a group IIIA or IVA element (Al, Ga, Si, and Ge) which is removed in the etching process, X represents carbon or nitrogen, and n varies from 1 to 4.[10] Usually, the as-prepared MXenes are endowed with abundant functional groups designated as T. For example, in $Ti_3C_2T_x$, the first and most-studied MXene,[8,11] T represents the surface terminating =O, –OH, and –F groups. Moreover, MXene features a variety of exceptional properties, including high electrical conductivity, good flexibility, defined surface groups T, adjustable hydrophilicity, and outstanding mechanical strength.[12] Over the past decade, more than 30 kinds of MXenes have been prepared on a lab scale[13] and extensively evaluated in energy storage,[11,14] electromagnetic shielding,[15] as sensors,[16] and membranes,[17] becoming one of the hottest current materials. As shown in Figure 1a–b, compared with other 2D materials such as graphene oxide (GO), transition metal dichalcogenides (TMDs), 2D zeolites, 2D metal–organic frameworks (MOFs), and 2D covalent-organic frameworks (COFs), MXenes are the fastest growing 2D material and also the fastest growing 2D membrane material, validated by the number of publications in the past two decades (Figure 1a–b). The special role of MXene in the family of 2D membranes was highlighted in a previous minireview.[17d]

Figure 1c shows some highlights of MXene membrane research. In 2014, MXenes started as an efficient Pb^{2+} adsorbent with an effluent Pb^{2+} concentration below the drinking water standard of 10 $\mu g\,L^{-1}$ (recommended by the World Health Organization), indicating the great potential of MXene in water purification.[18] Subsequently, MXenes have been extensively adopted for membrane separation, such as ion sieving,[19] gas separation,[20] desalination,[21] and organic solvent nanofiltration.[22] The TIMELINE of MXene membranes from 2014 to 2022 (Figure 1c) reflects the dynamic development of the different kinds of MXene membranes and their diverse applications in various separations.[17a–c,18–20,21a,23]

Since MXene is a superstar among emerging 2D materials, many reviews have summarized the potential applications of MXenes in the field of energy storage and

[*] L. Huang, L. Ding, H. Wang
Beijing Key Laboratory for Membrane Materials and Engineering, Department of Chemical Engineering, Tsinghua University
Beijing, 100084 (China)
E-mail: celiding@tsinghua.edu.cn
cehhwang@tsinghua.edu.cn

J. Caro
Institute of Physical Chemistry and Electrochemistry, Leibniz University Hannover
Callinstrasse 3A, 30167 Hannover (Germany)
E-mail: juergen.caro@pci.uni-hannover.de

clarified the underlying separation mechanisms.[24] However, MXene membranes also achieved excellent performance for drinking water production, but only a few studies[25] try to systematically review the latest progress and explain the fundamental mechanisms on a molecular level. Consequently, a comprehensive summary of MXene membranes for drinking water production is desirable for researchers to design more advanced membranes with better performance. In this review, we will focus on 1) the unique properties of MXenes, 2) the preparation of MXene membranes, 3) the applications of MXene membranes in water purification and the corresponding separating mechanisms, and 4) the remaining challenges and prospects for MXene membranes in drinking water production.

2. Adjustable properties of MXene nanosheets for water purification

Among the various 2D materials, such as GO, TMDs, 2D zeolites, 2D MOFs, and 2D COFs, the MXene nanosheets have some unique advantages over the others as a basic material of membranes for water purification. This chapter will briefly review the adjustable properties of MXenes in drinking water purification, including structural diversity, processibility, mechanical strength, antifouling resistance, and photothermal activity.

2.1. Diversity

Until now, over 30 different kinds of MXenes have been prepared experimentally, and over 100 kinds of MXenes have been predicted theoretically, which provide a huge reservoir for constructing high-performance MXene membranes.[13] The birth of $Ti_3C_2T_x$ nanosheets opened a new avenue for MXenes in the 2D materials world.[8] By using hydrofluoric (HF) acid to selectively extract the Al layer from the MAX phase Ti_3AlC_2, $Ti_3C_2T_x$ MXene nanosheets can be obtained (Figure 2a, b).[9a,13] Since then, HF has been widely used as the etchant[10c,26] to prepare MXene nanosheets. However, the direct use of HF acid results in defective MXene nanosheets and a low MXene yield due to the violent reaction.[14b] Besides, HF is highly corrosive and toxic. Therefore, new milder preparation methods are highly desired. In 2014, Ghidiu et al.[10b] demonstrated that by using in situ HF formed from LiF and HCl, MXenes can be prepared. The in situ etching method is milder and can produce high-quality MXene nanosheets. In addition, the

Lingzhi Huang is currently a Ph.D. candidate in the Department of Chemical Engineering at Tsinghua University, under the guidance of Prof. Haihui Wang. She received her Bachelor's degree in College of Materials Science and Engineering from Sichuan University in 2021. Her current research focuses on MXene-based membranes for separation applications.

Dr. Li Ding is an assistant research fellow at Department of Chemical Engineering, Tsinghua University. He received his Ph.D. degree from South China University of Technology in 2019, under the supervision of Prof. Haihui Wang. From 2019 to 2022, he continued his research at the South China University of Technology as a postdoctoral fellow. He joined Tsinghua University since August 2022. His current research focuses on two-dimensional membranes for efficient separation applications and mass transport in nanochannels. He has published over 20 papers at Nat. Sustain., Nat. Commun., Angew. Chem. Int. Ed., etc., with citation more than 2000.

Prof. Jürgen Caro studied Chemistry at Leipzig University and got Ph.D. in 1977. Until 1991 he worked at Institute of Physical Chemistry of Academy of Sciences of East Germany. From 1991 to 2001, he was at Institute of Applied Chemistry in Berlin-Adlershof in the fields inorganic and polymer materials, functional materials, reaction engineering. Since 2001, J. Caro was professor for Physical Chemistry at Leibniz University Hannover. From 2018–2021, he is distinguished Professor at School of Chemistry and Chemical Engineering at South China University of Technology, Guangzhou. J. Caro is member of the Saxon Academy of Sciences and Humanities at Leipzig.

Prof. Haihui Wang received his Ph.D. degree from the Chinese Academy of Sciences in 2003. After one year stay as an Alexander von Humboldt Research Fellow in the Institute of Physical Chemistry and Electrochemistry, Leibniz University Hannover, Germany, he continued his research there as a postdoctoral fellow from 2005. From 2007 to 2020, he worked at South China University of Technology. From November 2020, he is a full professor at Tsinghua University. His interests focus on inorganic membranes, membrane reactors, and energy materials. He has published over 240 papers at Nat. Energy, Nat. Sustain., Sci. Adv., etc., with citation of more than 20000.

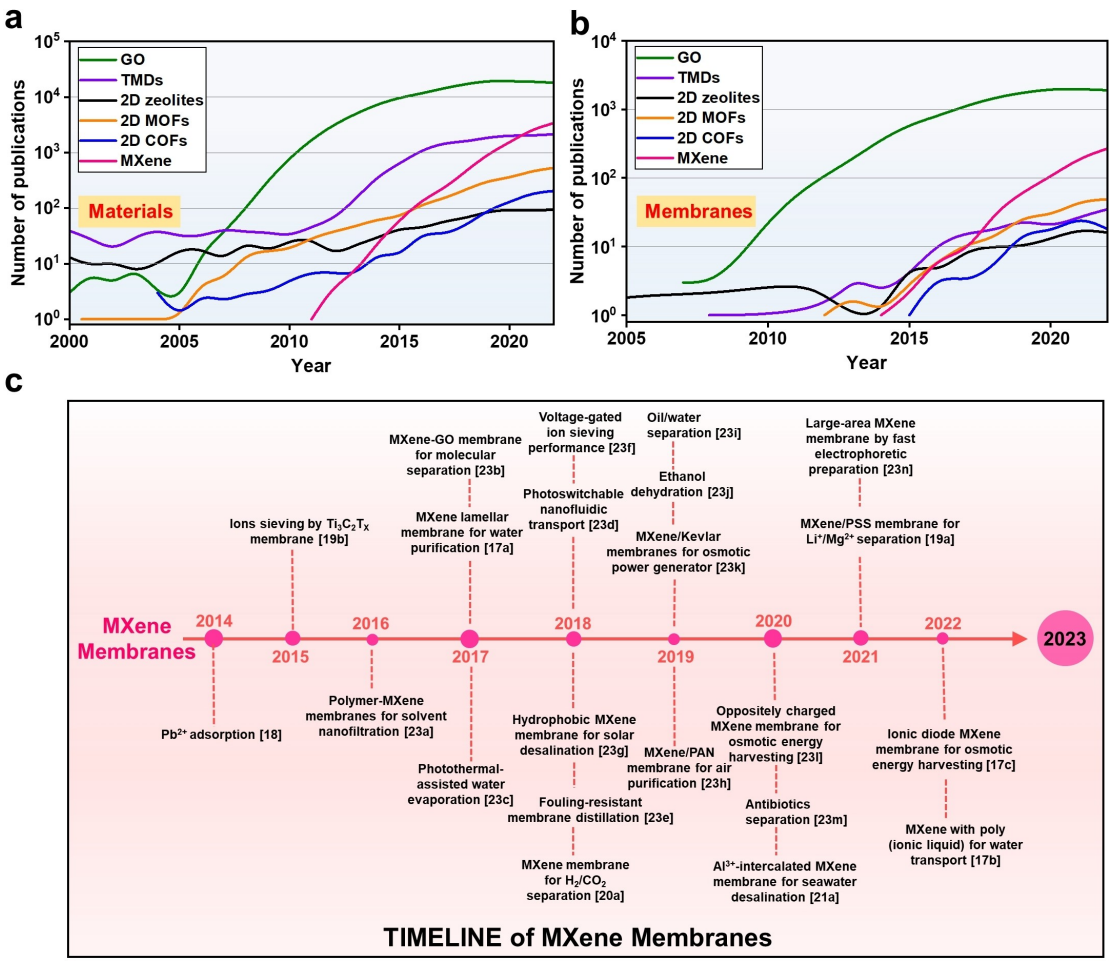

Figure 1. Number of publications on GO, TMDs, 2D zeolites, 2D MOFs, 2D COFs, and MXene as **(a)** materials and **(b)** membranes from 2000 to 2022 based on Web of Science databases. **(c)** TIMELINE of MXene membranes from 2014 to 2022.[17a–c,18–20,21a,23]

Li^+ ions could intercalate into the interlayers of the MAX and facilitate the delamination, which helps to obtain a higher MXene yield.[10b]

In fact, besides the HF etching process, there are also diverse other protocols to prepare MXene nanosheets,[27] including molten salt etching,[28] high-temperature alkali treatment,[29] and electrochemical etching,[30] which can be called Top-down methods. These methods unavoidably involve the steps of etching, delaminating, or sonicating, which might lead to a low quality of the MXene nanosheets. Accordingly, the Bottom-up methods, comprising chemical vapor deposition,[31] plasma-enhanced pulsed laser deposition,[32] and template method,[33] would be more suitable for preparing high-quality and uniform MXene nanosheets but with a much lower efficiency. However, despite the above big diversity, only two kinds of MXenes[21a,34] have been prepared so far as separation membranes, demonstrating the huge potential of MXenes still waiting to be discovered.

2.2. Processibility

Precise engineering of 2D nanomaterials such as GO[7c] or MXene[20a] enables the construction of high-performance separation membranes. Therefore, the processibility of nanosheets plays an important role in the membrane preparation process, especially their excellent dispersity and stability in aqueous solution.[8–9] Because MXene nanosheets are prepared mainly by etching and exfoliating processes in aqueous solutions, the surface of the MXene nanosheets usually contains abundant hydrophilic functional groups such as -OH, which is helpful to form and stabilize dispersions.[10a] After sonication and purification, the exfoliated MXene nanosheets can be easily dispersed in water with the observation of the Tyndall effect, indicating the formation of a stable and uniform colloidal solution. The most common way to prepare supported lamellar MXene membranes is vacuum-assisted filtration (VAF) on a porous substrate. Further, the excellent dispersity is conducive for functionalizing the MXene nanosheets for improved membranes fabrications. For instance, by tuning the concentration and lateral size (Figure 2c), liquid-crystalline (LC) MXene dispersion of high viscosity with oriented nanosheets

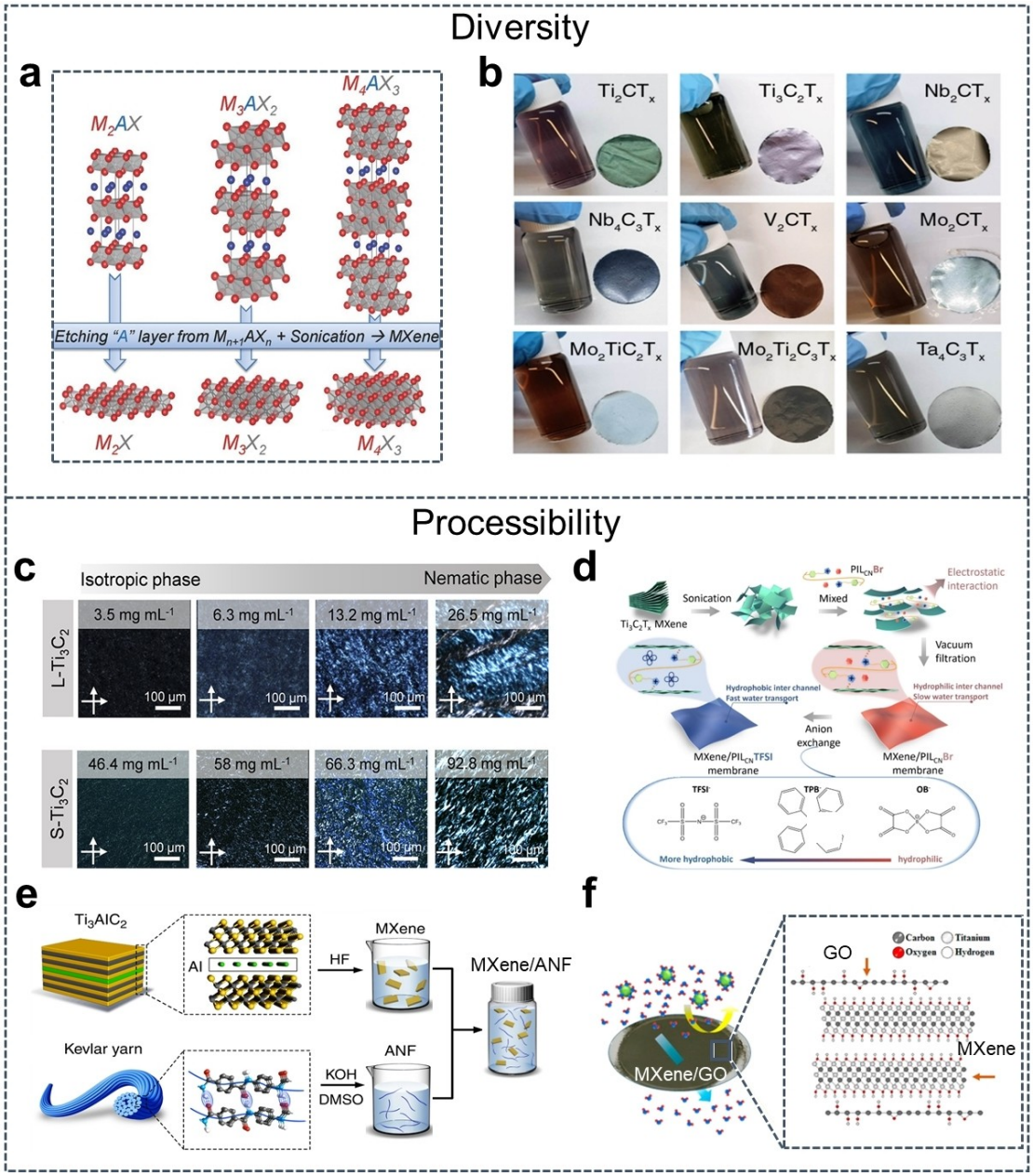

Figure 2. Diversity and processibility of MXenes. **(a)** Structures of MAX phases and corresponding MXenes. Reproduced with permission.[9a] Copyright 2014, Wiley-VCH. **(b)** Various MXene dispersions and the corresponding MXenes films. Reproduced with permission.[13] Copyright 2021, The American Association for the Advancement of Science. **(c)** Birefringence changes of $Ti_3C_2T_x$ inks at increasing concentrations demonstrating the transformation from isotropic to nematic phase. Reproduced with permission.[35b] Copyright 2020, American Chemical Society. **(d)** Formation of Poly(ionic liquid)/MXene composite lamellar membrane. Reproduced with permission.[17b] Copyright 2022, Wiley-VCH. **(e)** Composite formation of MXene nanosheets and Aramid nanofibers (ANF). Reproduced with permission.[23k] Copyright 2019, Nature Publishing Group. **(f)** Illustration of the GO/MXene composite membrane for molecular separation. Reproduced with permission.[23b] Copyright 2017, American Chemical Society.

could be obtained.[35] According to a previous report, using LC nanosheet dispersion is helpful to prepare supported lamellar membranes with ultrahigh stacking order with superior separation performance.[36] Besides, the stable nanosheet dispersion allows us to pre-modify the nanosheet and blend them with other functional materials. For example, through treatment with trimethoxy(perfluorodecyl)silane (PFDTMS), the hydrophilic MXene nanosheets become hydrophobic, which enhances the salt-blocking ability of the corresponding MXene membrane.[23g] Moreover, the coupling of MXene nanosheets with other materials is quite simple due to the high compatibility and dispersity of MXene nanosheets. Composite MXene lamellar membranes (Figure 2d–f) are commonly evaluated in water treatment, such as Poly(ionic liquid)/MXene,[17b] Kevlar/MXene,[23k] nanoparticles (NPs)/MXene,[23e] and GO/MXene.[23b] In conclusion, the good processibility of MXenes facilitates the fabrication of

MXene membranes and helps to extend the application of MXenes.

2.3. Mechanical property

Both supported lamellar MXene membranes as well as Mixed Matrix Membranes (MMMs) need sufficient mechanical properties for water purification because these membrane processes such as microfiltration, ultrafiltration, reverse osmosis, and nanofiltration are usually operated under pressure-driven conditions. The mechanical property of the MXene nanosheets and their assembly behavior directly influence the mechanical strength of MXene-based membranes. However, the exploration of MXene's mechanical properties is at the early stage, only two kinds of MXene nanosheets have been experimentally tested so far.[12] The elastic properties of $Ti_3C_2T_x$ monolayers[12b] were measured by Atomic Force Microscopy (AFM), demonstrating an ultrahigh Young's modulus of ≈330 GPa (Figure 3a). Similarly, Young's modulus of $Nb_4C_3T_x$ nanosheets[12a] was around 386 GPa, the highest value reported so far for nanoindentation measurements of solution-processable 2D materials. However, due to the weak interaction and disordered stacking of MXene nanosheets, the pristine supported MXene membrane obtained by VAF showed poor mechanical strength with a tensile stress of only ≈40 MPa.[35c] Incorporating chain polymers is helpful to further enhance the mechanical strength of MXene-based membranes.[37] For example, an MXene/Kevlar nanofiber composite membrane[23k] reached a high tensile stress of ≈101 MPa, which is comparable to natural nacre. This finding is attributed to the Kevlar nanofibers serving as interlocking agents to strengthen the interactions between the MXene nanosheets through strong hydrogen bonding. Besides, by enhancing the stacking order of MXene nanosheets, the corresponding mechanical strength of MXene membranes can be greatly improved. For instance, Wang et al.[35c] reported a 940 nm thick $Ti_3C_2T_x$ film that exhibited record tensile stress over 570 MPa prepared by the blade-coating method. The applied shear force brought about by the blade causes an almost perfect stack-like orientation of the MXene nanosheets, which largely improves the mechanical strength (Figure 3b, c).[35c]

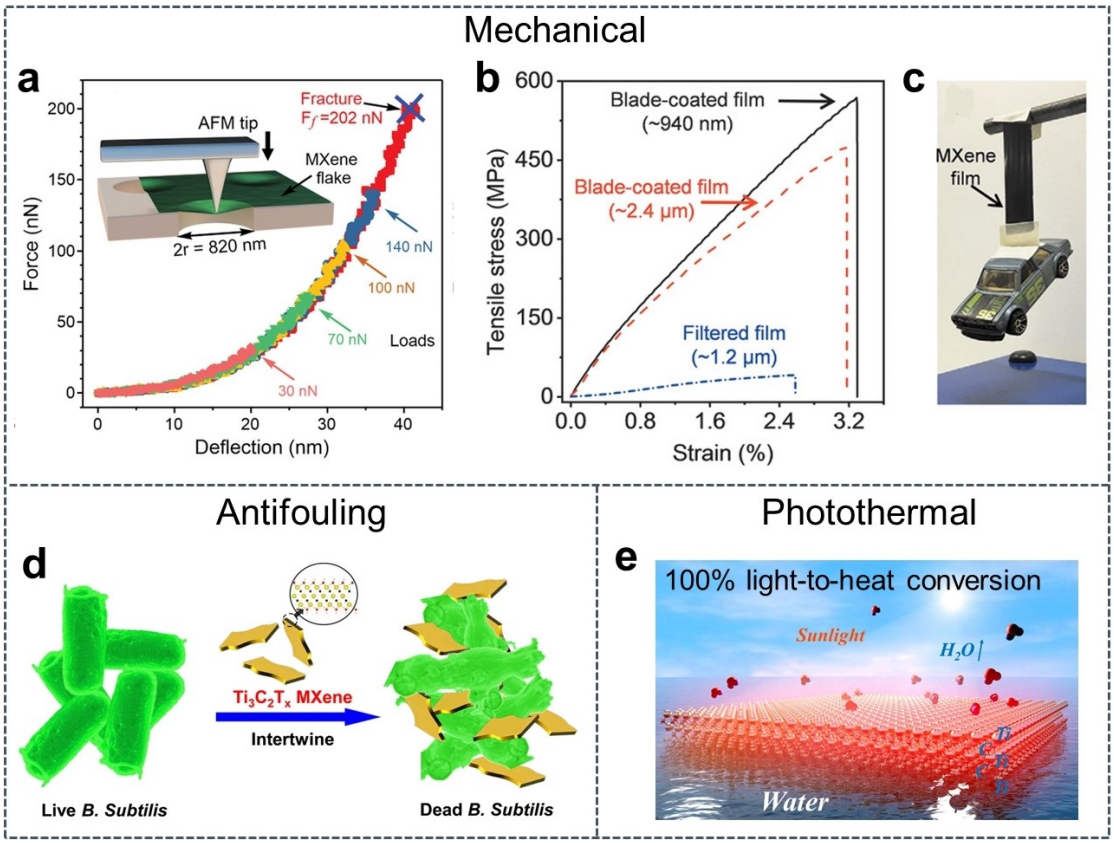

Figure 3. Mechanical, antifouling, and photothermal properties of MXenes. **(a)** Mechanical property of MXene flake measured by AFM. Reproduced with permission.[12a] Copyright 2020, Wiley-VCH. **(b)** Tensile stress of the blade-coated MXene film, and **(c)** the corresponding digital photo of the ultra-strong MXene film. Reproduced with permission.[35c] Copyright 2020, Wiley-VCH. **(d)** Antibacterial ability of MXene, which leads to the activity loss of B. subtilis. Reproduced with permission.[39] Copyright 2016, American Chemical Society. **(e)** Excellent light-to-heat capability of MXene with 100% conversion efficiency. Reproduced with permission.[23c] Copyright 2017, American Chemical Society.

2.4. Antifouling property

Another important criterion of membranes in water purification is their antifouling resistance against salts, organics, and microorganisms.[38] Antifouling-resistant membranes avoid frequent replacement, thus extending their lifetime and saving costs. In 2016, the antibacterial activity (Figure 3d) of $Ti_3C_2T_x$ MXene nanosheets was first investigated..[39] Remarkably, over 98 % of the bacteria Escherichia coli (E. coli) and Bacillus subtilis (B. subtilis) cells lost viability within 4 h of exposure to a 200 $\mu g\,mL^{-1}$ $Ti_3C_2T_x$ MXene solution while the GO only induced ≈90 % inactivation at the same concentration. This finding demonstrates the outstanding antibacterial ability of $Ti_3C_2T_x$ is attributed to the damage to the bacteria's cell membrane, leading to the release of cytoplasmic materials.[39] Recent reports have shown that composites of MXenes and NPs further enhance the antibacterial effect. For example, Pandey et al.[23e] combined Ag NPs and MXene nanosheets to prepare an Ag/MXene composite membrane for fouling-resistant separation. The composite membrane could inhibit the growth of E. coli over 99 %, which is a great improvement compared with the pristine MXene membrane (≈60 %). Moreover, a heterostructure composite of ZnO/$Ti_3C_2T_x$ was prepared as a high-efficiency antibacterial and antibiofilm, reaching a 100 % sterilization effect.[40]

Notably, the hydrophilic nature of MXene nanosheets[9a] favors the self-cleaning of MXene against oil or other organic pollutants,[23i,41] which is beneficial for the development of antifouling MXene membranes for oil/water emulsion separation.[41a] Besides, the high processibility of MXene nanosheets allows tuning the hydrophilicity of MXene nanosheets to prevent salt crystallization on their surface during evaporation. For instance, the PFDTMS-modified hydrophobic MXene membrane[23g] achieved an evaporation rate of 1.3 $kg\,m^{-2}\,h^{-1}$ and stable performance over 200 hours with excellent salt-blocking resistance even under high salinity conditions.

2.5. Photothermal ability

Thermally-driven membrane distillation including solar evaporation is a promising process to purify seawater.[42] Under solar irradiation, it is very advantageous if the membrane shows an effective light-to-heat conversion so that the energy input can be remarkably reduced and the total energy conversion can be significantly improved.[43] MXenes are very suitable for this light-to-heat harvesting since they show a high electromagnetic interference (EMI) shielding effect,[44] which is related to the prominent absorption ability of MXenes. The perfect electromagnetic wave absorption of MXenes guides researchers to investigate the absorption ability of sunlight and the corresponding heat conversion. In 2017, Li et al.[23c] first explored the internal light-to-heat transformation of $Ti_3C_2T_x$ and found that $Ti_3C_2T_x$ can completely convert light to heat (Figure 3e), namely with an almost 100 % light-to-heat conversion, which is higher than that of the well-known carbon nanotubes (CNTs).[23c] Further, they tested the efficiency of $Ti_3C_2T_x$ membranes for interfacial steam generation and achieved a light-to-water-evaporation efficiency of ≈84 % under sunlight illumination (1 $kW\,m^{-2}$), opening the avenue of MXenes in thermally-driven distillation.[23c]

3. Preparation of MXene membranes

Generally, 2D membranes can be classified into nanosheet membranes with in-plane porosity and lamellar membrane stacks without porosity in the nanosheets.[6c] The nanosheet membranes usually consist of a single or a few layers of nanosheets with in-plane porosity which controls molecular transport through the intrinsic or post-synthetic created pores. The lamellar non-porous membranes consist of stacked impermeable nanosheets, and molecular transport takes place through the interlayer between the nanosheets.[6b] However, so far it was too difficult to synthesize porous MXene nanosheets or to create post-synthetic porosity. Consequently, the current MXene membranes are confined to lamellar stacks of non-porous nanosheets or incorporate MXene nanosheets into a polymer matrix (MMMs).[45] The lamellar membranes consist of stacked MXene nanosheets, exhibiting the classic layer-by-layer stacking structure of 2D membranes. While in MMMs, the MXene nanosheets usually act as the fillers, while the polymers act as the continuous body of the membranes. Therefore, based on the structure, the preparation methods for MXene-based membranes will be divided into two parts, lamellar non-porous nanosheet membranes and MMMs.

3.1. Lamellar membranes

The stacking order of the nanosheets in the lamellar membranes plays a critical role in their separation performance.[36] VAF is the most common method for preparing supported lamellar membranes. The abundant surface functionalities T such as =O and –OH in the formula $Ti_3C_2T_x$ give the MXene nanosheets hydrophilicity,[8] which makes it easy to obtain stable and uniform aqueous MXene dispersions. Typically, the alignment of nanosheets can be affected by the quality of the nanosheets, their uniformity and concentration of the dispersion, the pressure gradient, and the substrates used in VAF. For instance, after etching and sonication, the delaminated MXene nanosheets could be uniformly dispersed in water. Then, a certain amount of the dispersion is filtered on porous substrates (Poly(vinylidene fluoride) (PVDF),[19b] Poly(ether sulfones) (PES),[19a] AAO(Anodic Aluminum Oxide),[17a] etc.) for preparing supported MXene membranes (Figure 4a).[36] The as-prepared MXene membrane shows an aligned structure with only a few defects or non-selective pores which is conducive to efficient separation. Furthermore, VAF is also extensively applied in preparing composite MMMs by mixing MXene nanosheets with dissolved polymers or other materials, such as MXene/poly(sodium 4-styrene sulfonate) (PSS),[19a] MXene/poly(vinyl alcohol) (PVA),[46] MXene/

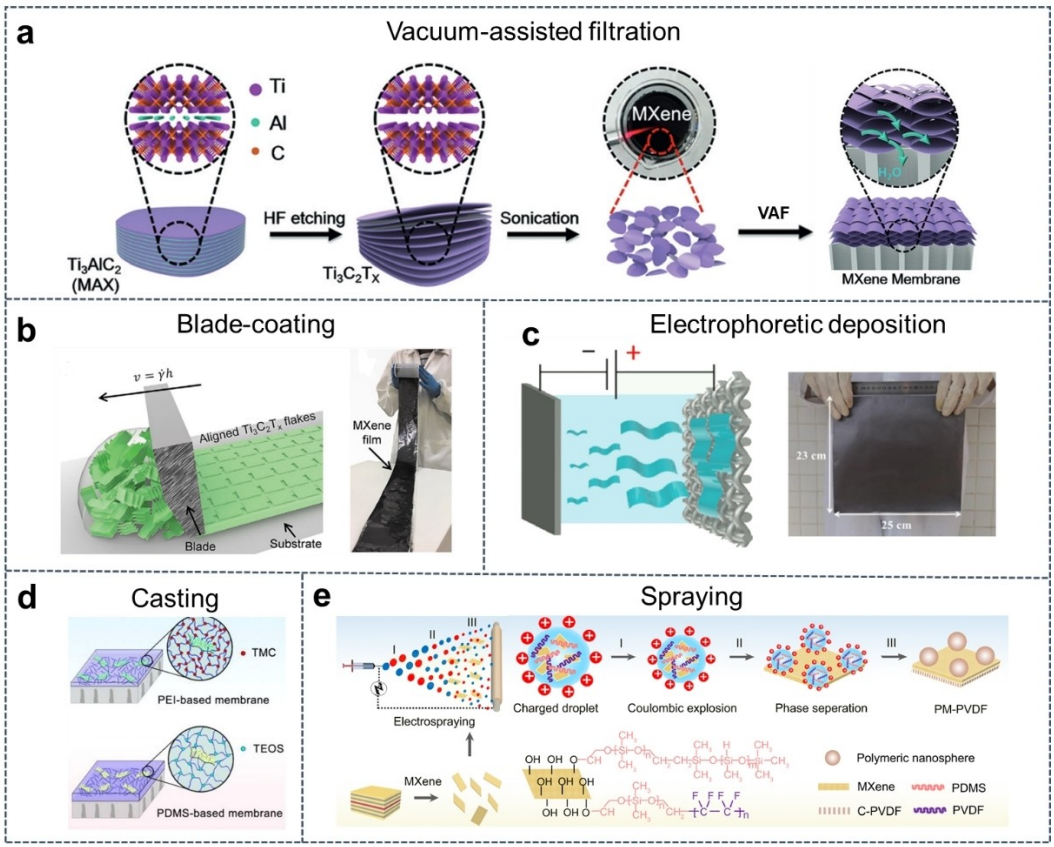

Figure 4. Preparation methods of MXene membranes. **(a)** Illustrations of the VAF method. Reproduced with permission.[17a] Copyright 2017, Wiley-VCH. **(b)** Blade-coating method. Reproduced with permission.[35c] Copyright 2020, Wiley-VCH. **(c)** Electrophoretic depositionfor preparing large-area MXene membranes. Reproduced with permission.[23n] Copyright 2021, Elsevier. **(d)** Casting MMMs with functionalized MXene nanosheets on PAN substrates. Reproduced with permission.[49] Copyright 2017, Elsevier. **(e)** Electrospraying of MXene nanosheets on polymer supports. Reproduced with permission.[50] Copyright 2022, Nature Publishing Group.

polyethyleneimine (PEI),[47] MXene/GO,[23b] and MXene/CNTs.[48]

Compared to VAF, the blade-coating method can facilitate and improve the stacking order of lamellar membranes but it needs a high-concentration slurry.[36,51] According to recent reports, nanosheet dispersions in the nematic phase[51] are desirable to get super-aligned MXene membranes. The oriented nanosheets in the dispersion and the shear force applied to the dispersion in the blade-assisted layer formation, both effects the parallel arrangement of the nanosheets. For example, Zhang et al.[35c] prepared a freestanding and mechanically strong MXene film by using the blade coating method with a nematic MXene nanosheet dispersion (Figure 4b). It should be mentioned that blade-coating is also suitable for large-scale production. Electrophoretic deposition[23n] (Figure 4c) can be also applied to prepare large-area MXene membranes within 10 min. This technique is based on electrostatic attraction. The negatively charged MXene nanosheets can be directly deposited on the anode under the electric field.[23n] Although these methods have been widely and successfully used in labs, the continuity of the process and the defects in the membranes should be considered when facing large-scale production.

3.2. MMMs

Besides being stacked as functional lamellar membranes, MXene nanosheets can also serve as fillers in MMMs.[52] Different from the supported lamellar membranes, the stability of the MMMs is improved dramatically due to the continuous polymer phase functioning as the matrix, providing better anti-swelling capability and higher mechanical strength.[53] So far, casting[23a,54] and coating (such as dip-coating, spray coating, spin-coating, and blade-coating)[50,55] are mostly used to construct MMMs. For example, Hao et al.[49] first grafted four different functional groups on MXene nanosheets to make them compatible with polymer solutions of PEI or polydimethylsiloxane. The composite suspension was drop-casted on a polyacrylonitrile (PAN) substrate (Figure 4d) to fabricate MMMs for solvent nanofiltration.[49] Moreover, MXene nanosheets also have been successfully incorporated into PES,[45b,56] polysulfone (PSF),[54] polyamide (PA),[57] and PAN[58] to construct MMMs for water purification. For instance, Zhu et al.[57] brushed MXene nanosheets on the PES support to assist the interfacial polymerization of PA and found an enhanced nanofiltration performance. Yao et al.[56] incorporated ZIF-8 together with $Ti_3C_2T_x$ into a PES matrix and prepared

MMMs by the casting method for efficient dye/salt separation. Moreover, spraying is also applied to form MMMs. Recently, Zhang et al.[50] prepared MXene-polymer MMMs by a facile electrospray process (Figure 4e) and evaluated the MMMs in membrane distillation for desalination. Here, the functionalized MXene nanosheets exploit the photothermal effect and show strong water-repellency owing to the transformation from intrinsic hydrophilicity into superhydrophobicity.

4. MXene membranes for water purifications

Generally, the pollutants in wastewater can be classified according to their size: Micrometer, nanometer, and sub-nanometer, as shown in Figure 5. In the past decade, various types of MXene membranes have been applied for drinking water purification and achieved excellent separation performance.[17b,50,59] To clearly understand the development of MXene membranes for water purification, we will systematically discuss the research progress by the classification of the pollutants' size, starting with the separation mechanism.

4.1. Separation mechanisms

Currently, there are mainly two kinds of MXene membranes under study, supported lamellar membranes and MMMs which can be self-supporting or supported.[60] The former lamellar membranes are constructed by self-stacking MXene nanosheets, mainly deposited by VAF. Generally, there are two kinds of interactions inside the lamellar membranes. One is the attractive Van der Waals force between nanosheets, the other is the electrostatic repulsion due to the same negative surface charge of the MXene nanosheets. Consequently, there exists a certain distance between adjacent nanosheets as an equilibrium state of forces, forming a slit-shaped 2D nanochannel as free spacing between the nanosheets.[19b] In a pioneering paper, the interlamellar distance between the MXene nanosheets could be chemically tuned for selective H_2 or CO_2 transport via molecular sieving and adsorption. Borate and PEI could control the stacking and interlayer spacing.[20b] Since the majority of MXene membranes use $Ti_3C_2T_x$,[21b,52,61] the following discussions are focused on $Ti_3C_2T_x$-type membranes. Typically, the pristine MXene membranes exhibit a free-spacing of ≈3.5 Å in the dry state, but the free-spacing increases to ≈6 Å in the wet state.[19] The expansion of the free spacing is mainly attributed to the intercalation of water molecules between adjacent MXene layers in aqueous solutions.[19b,21a] Therefore, in the water purification environment, the effective channel size of MXene membranes is ≈6 Å, which is much smaller than bacteria, pharmaceuticals, hormones, dyes, and NPs, so these impurities can be effectively removed (Figure 6a).[25,62] In 2015, Ren et al.[19b] first verified that an MXene membrane prepared by VAF can effectively reject methylene blue (MB, ≈9.7 Å) through size exclusion with a water permeance of 37.4 $L\,m^{-2}\,h^{-1}\,bar^{-1}$.

Besides, the abundant surface groups (=O, –OH, and –F) of the MXene nanosheets provide a negative surface charge (Zeta potential, around −35 mV)[17a,22,63] in aqueous solution. These negative groups play an important role in ion sieving due to electrostatic rejection (Figure 6b).[21b,23d,f,64] Importantly, the monovalent ions (Li^+, Na^+, K^+) are more likely to pass through the membranes, while the multivalent ions (Mg^{2+}, Ca^{2+}, Al^{3+}) tend to adsorb at the surface due to the strong electrostatic attraction.[21a] This phenomenon demonstrates the enormous potential of MXene membranes in mono/multivalent ion sieving. Moreover, the surface charge density can be easily tuned through materials combination, such as with ANF,[23k] CNTs,[58,65] PSS,[19a] or by charge reversal through adsorption of poly(diallyldimethylammonium chloride) (PDDA).[17c] Recently, the Wang group revealed the potential of the MXene membrane in separating Li^+/Mg^{2+} by increasing the charge density of the MXene channels through the incorporation of PSS.[19a] Additionally, the negative charge and high specific surface area endow MXenes with excellent adsorption capability for heavy metals, such as Pb^{2+}, Ba^{2+}, Sr^{2+}, Cd^{2+}, U^{6+}, and

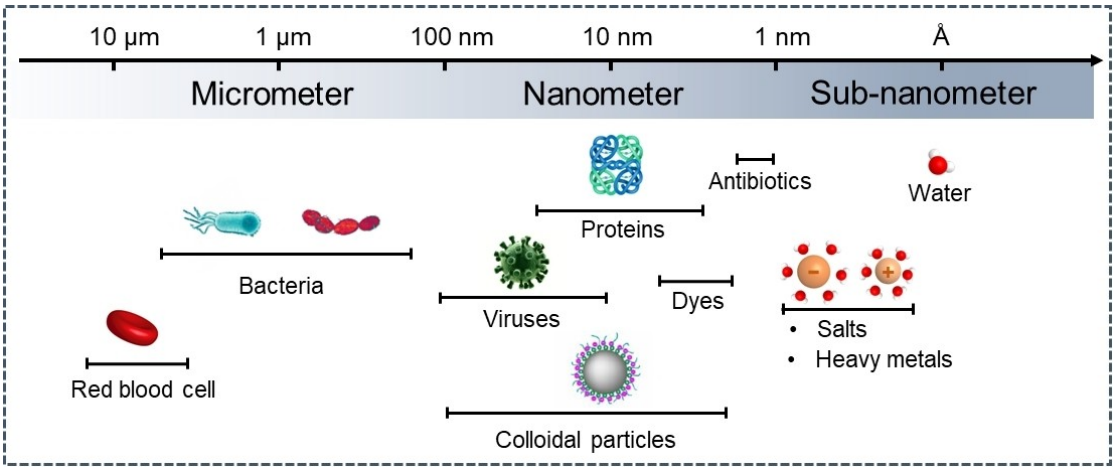

Figure 5. Illustration of pollutants in water based on different sizes, from micrometer to sub-nanometer.

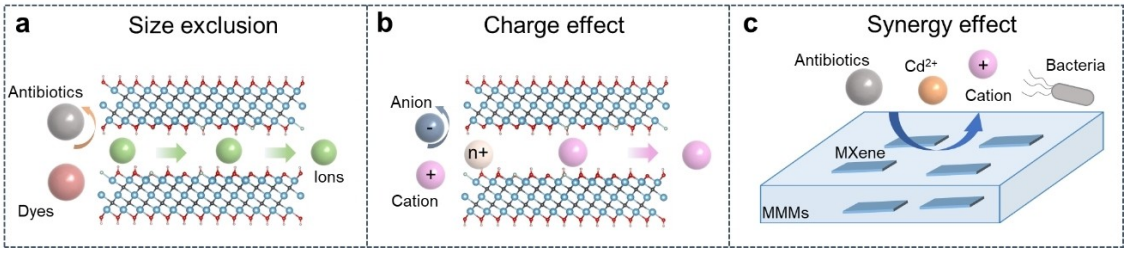

Figure 6. Separation mechanisms of molecules and ions through MXene-based membranes. **(a)** Size effect, **(b)** charge effect, and **(c)** synergy effects.

Re^{7+}.[18,66] The abundant positive charges and large sizes tend to be adsorbed at the MXene surface, contributing to the ultraslow permeation rate. Therefore, removing heavy metal ions mainly attributes to the adsorption capability of MXene nanosheets. For example, Peng et al.[18] reported the unique Pb^{2+} adsorption behavior of $Ti_3C_2T_x$, the sorption equilibrium was quickly achieved after 120 s and the effluent Pb^{2+} content is below the drinking water standard of $10\,ug\,L^{-1}$, indicating the excellent heavy metal adsorption ability of MXene.

For MMMs, the separation mechanisms (Figure 6c) are more complex.[67] First, the added MXene nanosheets influence the length of the transport pathways for molecules through the polymer, thus facilitating the fast and precise sieving process.[60a] Second, the abundant terminating groups T on the MXene surface also play an essential role in separating charged molecules through electrostatic interactions and pore narrowing. Third, the polymer matrix can separate molecules through the solution-diffusion mechanism and/or the Donnan effect. Further, the presence of nanomaterials like MXene nanosheets modifies the molecular structure of the polymer and so its permeation behavior.[68] Therefore, the synergistic effects of MXene nanosheets and polymer matrix can push an efficient separation.[69]

4.2. Micrometer impurities: Bacteria

Due to their relative size, bacteria can be easily separated using membranes. However, the deposition and physical adsorption of microorganisms such as bacteria, algae, protozoa, and fungi causes a biofilm formation which can block water permeation. This biofouling has always been an inevitable issue in water purification because the complex water environment provides a breeding ground for bacterial reproduction. The excellent antibacterial ability of MXenes feeds the hope to prepare bacteria-selective antifouling membranes with longtime stable separation performance.[23e,70] Previous reports have found that the sharp edge of MXene nanosheets can damage the cell membrane of bacteria, thus killing the bacteria and inhibiting their growth, which signifies the excellent antibacterial ability of MXenes.[39,71] However, the antibacterial ability of the MXene membrane can significantly decrease because of the decreased surface area after membrane assembly.[23e] As shown previously, incorporating Ag NPs into the MXene lamellar membrane remarkably enhances their antibacterial properties. The composite Ag@MXene membrane (Figure 7a–b) could inhibit 99 % E. coli growth, which is much higher than that of the pristine MXene membrane (60 %).[23e] Moreover, the Ag NPs widen the transport pathways for water molecules through the interlayers of the MXene nanosheets, and the water permeance increases from $\approx 118\,L\,m^{-2}\,h^{-1}\,bar^{-1}$ to $\approx 420\,L\,m^{-2}\,h^{-1}\,bar^{-1}$. Recently, the same strategy was adopted to synthesize Ag@MXene/PEN (poly(arylene ether nitrile)) composite lamellar membrane[70] to further improve the water permeance to more than $10{,}000\,L\,m^{-2}\,h^{-1}\,bar^{-1}$ without sacrificing the antibacterial ability ($\approx$99.9 % E. coli growth inhibition), as shown in Figure 7c.

4.3. Nanometer impurities: Organic pollutants

Organic pollutants such as pharmaceuticals, hormones, pesticides, and antibiotics, are typical contaminants in wastewater, which can devastate our ecosystem heavily.[72] The efficient removal of these organic pollutants is crucial for drinking water production as well as the whole ecosystem. The use of membranes is especially reasonable for highly concentrated effluents near the polluters, i.e., pharma or agrochemical companies, hospitals, etc. These organic pollutants are usually at the nanometer sizes, from one nanometer to several nanometers.[73] Hence, the lamellar MXene membranes with a channel size of $\approx$6 Å can exclude them perfectly with super high rejection rates. However, the water flux is relatively low, far from meeting the demand of practical applications. To improve the water permeance, the Wang group proposed the "pore widening" strategy to expand the channels. The results indicate that the expanded channels significantly increase the water permeance without sacrificing the rejection rates.[17a] In detail, $Fe(OH)_3$ colloidal particles were chosen to intercalate the MXene nanosheets, followed by the VAF method to prepare the membrane. Afterward, the $Fe(OH)_3$ particles were removed by dissolving them with hydrochloric acid (HCl).[17a] The porous MXene membrane's water permeance (Figure 7d) has been improved about 5–10 times compared with the pristine MXene membrane, reaching an ultrahigh permeance of $1{,}000\,L\,m^{-2}\,h^{-1}\,bar^{-1}$. Impressively, the rejection of various proteins and dyes remained unchanged. For example, the

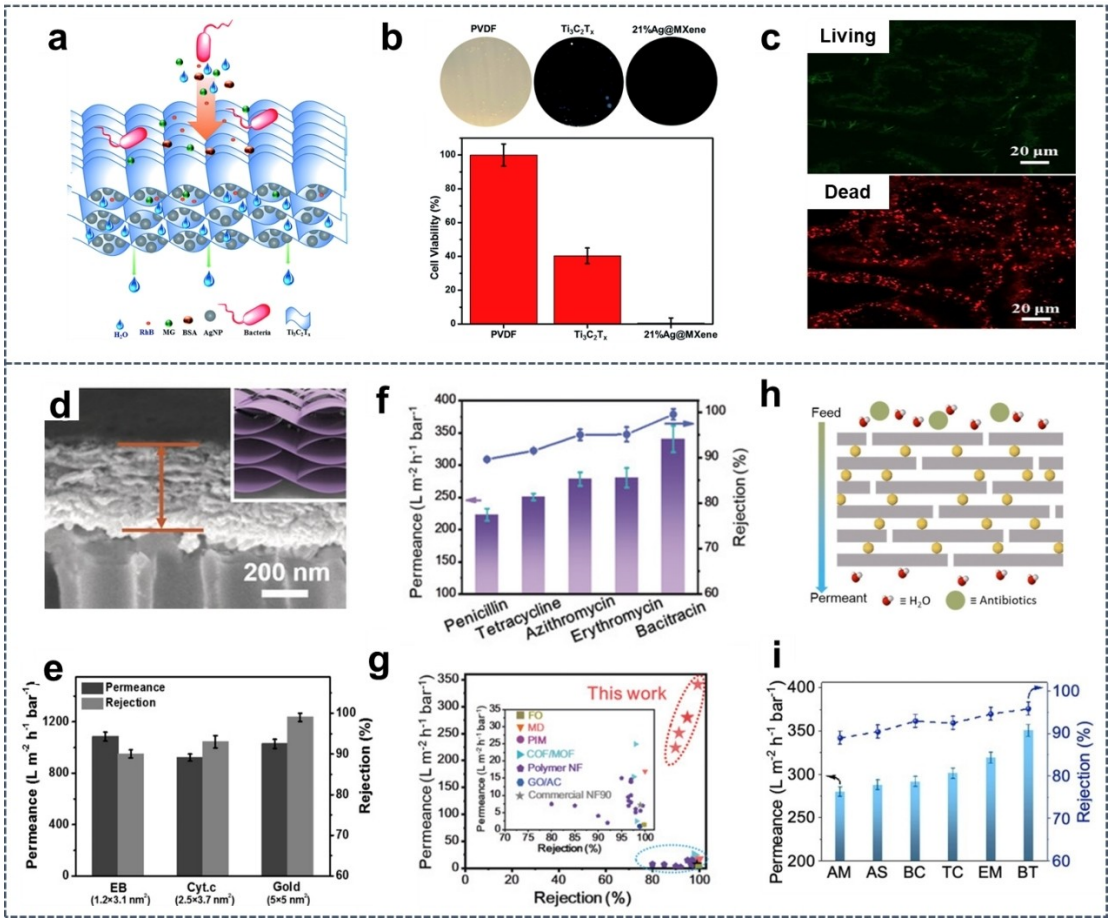

Figure 7. MXene membranes for bacteria, dyes, and antibiotics rejection. **(a)** Schematic structure and rejection mechanism of the 21 % Ag@MXene composite membrane. **(b)** Antibacterial activity of PVDF, MXene ($Ti_3C_2T_x$), and Ag@MXene membranes. Reproduced with permission.[23e] Copyright 2018, Royal Society of Chemistry. **(c)** Comparisons of living and dead E. coli cells for Ag@MXene/PEN composite membrane. Reproduced with permission.[70] Copyright 2022, Elsevier. **(d)** Cross-sectional Scanning Electron Microscopy (SEM) image and **(e)** Separation performance of the MXene membrane. Reproduced with permission.[17a] Copyright 2017, Wiley-VCH. **(f)** Antibiotics separation performance of MXene membrane and **(g)** Comparisons with other reports. Reproduced with permission.[23m] Copyright 2020, Wiley-VCH. **(h)** Illustration of the MXene-pillararene membrane and **(i)** Corresponding separation performance of antibiotics. Reproduced with permission.[59c] Copyright 2022, Wiley-VCH.

rejection rate of bovine serum albumin (BSA) was unchanged nearly 100 %. Although the rejection decreased a little for smaller dye molecules, such as Cytochrome (Cyt. c, 97 %, 2.5×3.7 nm^2), EB (Evans blue, 90 %, 1.2×3.1 nm^2), and rhodamine B (RhB, 85 %, 1.8×1.4 nm^2), the separation performance of the porous membrane after $Fe(OH)_3$ extraction is still outstanding (Figure 7e). Besides widening the distance between the nanosheets of the MXene membrane, modifying the channels′ microenvironment also has proved to be an efficient way to facilitate water transport. Modification of the MXene nanosheets with $–NH_2$ makes the membrane hydrophilic[22] and increases the water permeance to 1,563 L m^{-2} h^{-1} bar^{-1} with a moderate MB rejection rate of over 92 %. The comparisons of various MXene membranes according to their separation performance of organic pollutants is shown in Table 1.

A defect-free MXene membrane is strictly required for the separation of antibiotics since their sizes are usually smaller than hormones, pesticides, or dyes. Therefore, the Wang group prepared large MXene nanosheets with 2–4 μm lateral size to reduce defects in the stack.[23m] The as-prepared MXene membrane has a highly-ordered stacking of nanosheets with a super regular structure. Accordingly, the rejection rate for one of the smallest antibiotics penicillin (1.4×0.7 nm^2) achieved up to 89.5 % with a water permeance of ≈223 L m^{-2} h^{-1} bar^{-1}. Rejection rates of larger antibiotics such as tetracycline, erythromycin, azithromycin, and bacitracin, achieved 91.5 %, 95 %, 95.1 %, and 99.5 %, respectively, which outperform the state-of-the-art membranes (Figure 7f–g).[23m] To further improve the permeance, an inorganic-organic hybrid MXene-pillararene membrane was prepared to separate antibiotics, as shown in Table 1. The organic pillararene could increase the lateral size of the MXene nanosheets and enlarge the *d*-spacing, which allows fast transport of water molecules thus significantly improving the water permeance (Figure 7h–i).[59c]

Table 1: Comparison of MXene membranes separating organic pollutants.

Membrane type	Pollutant	Water permeance ($L m^{-2} h^{-1} bar^{-1}$)	Rejection rate (%)	Thickness	Ref.
Lamellar MXene membrane	MB	37.4	≈100	1.5 μm	[19b]
Lamellar MXene membrane	BSA	790	≈100	400 nm	[17a]
	Cyt. c	1056	97.0		
	EB	1084	90.0		
	RhB	806	85.0		
	TMPyP	921	93.0		
MXene-NH_2 membrane	MO*	1563	73.0	337 nm	[22]
	MB		92.0		
MXene/PIL_{CN}TFSI	RB*	420.4	96.1	225 nm	[17b]
	BT*	350.1	99.5		
COF/MXene	CR*	563	99.6	110 nm	[74]
21 % Ag/MXene composite membrane	BSA	345.8	≈100	470 nm	[23e]
	RhB	387.1	79.9		
	MG	354.3	92.3		
MXene/cellulose acetate MMMs	BSA	256.9	≈100	123 μm	[61]
	RhB		92.0		
	MG		98.0		
Lamellar MXene membrane	Penicillin	223.1	89.5	500 nm	[23m]
	Tetracycline	250.4	91.5		
	Erythromycin	278.5	95.0		
	Azithromycin	280.4	95.1		
	Bacitracin	340.5	99.5		
MXene-pillararene membrane	Penicillin	350.3	95.8	11 μm	[59c]
	Ampicillin	279.6	88.9		
	Ampicillin sodium	287.5	90.4		
	Erythromycin	291.2	92.9		
	Tetracycline	300.8	92.5		
	Berberine chloride	318.8	94.6		
	Bacitracin	350.3	95.8		
g-C_3N_4@MXene membrane	Tetracycline hydrochloride	1790	86.0	29 μm	[75]

MO*: Methyl Orange RB*: Rose Bengal CR*: Congo Red BT*: Eriochrome Black T

4.4. Sub-nanometer impurities: Salts and heavy metals

Besides the relatively large organic molecules mentioned above, also salts and heavy metal ions play an important role in purifying wastewater and seawater since they are difficult to separate due to their smaller sizes and similar valences.[76] So far, seawater distillation is one of the most effective approaches to produce drinkable and clean water owing to the abundant resource.[77] For most 2D membranes, swelling in aqueous solution is unavoidable because of the intercalation of water molecules. Accordingly, the interlayer *d*-spacing of MXene membranes expands to ≈6 Å in an aqueous media, which is close to the diameters of the hydrated ions like Na^+ (7.16 Å), or K^+ (6.62 Å).[78] Consequently, pristine MXene membranes could not exhibit a satisfying desalination performance due to swelling. Therefore, suppressing the swelling of the MXene membranes in water is the key to obtain high salt rejection.

Exploiting the abundant functional groups on the MXene nanosheet surface, the Wang group proposed an Al^{3+}-intercalating method (Figure 8a) to suppress the swelling by forming Al–O bonds.[21a] As displayed in Figure 8b–c, the cross-sectional SEM image and the high-angle annular dark-field (HAADF) confirm the continuous lamellar structure of the Al^{3+}-intercalated MXene membrane, and the element mapping demonstrates a uniform distribution of Al^{3+} in the MXene membrane. Accordingly, as shown in Figure 8d, the *d*-spacing of the intercalated membrane was confined to ≈5 Å in various aqueous solutions.[21a] As expected, the permeation of ions was strongly impeded, however, with water permeation rates reduced by more than 50 times (Figure 8e). Moreover, the water permeance of the Al^{3+}-intercalated MXene membrane still reached a flux of 2.8 $L m^{-2} h^{-1}$ with a NaCl rejection rate of over 96 % (Figure 8e inset). Importantly, the membrane shows superior stability in a 400 h long-term test (Figure 8f), exhibiting enormous potential in the practical desalination process.[21a] Using an ultrathin MXene membrane of 60 nm thickness, relative high water fluxes of 85.4 $1 m^{-2} h^{-1}$ with 99.5 % NaCl rejection at 65 °C could be obtained in pervaporation desalination.[80]

Solar-driven distillation is another key membrane technique to desalinate seawater by utilizing sun light as a natural heat source.[43a,81] It is well-known that MXenes are at the top of the list of light-to-heat materials with nearly perfect photothermal conversion.[13] Accordingly, in 2017, the MXene membranes achieved a light-to-water evaporation efficiency of 84 % under sun irradiation, demonstrating for the first time the huge potential of MXenes in solar-driven desalination.[23c] Afterwards, a series of studies were pub-

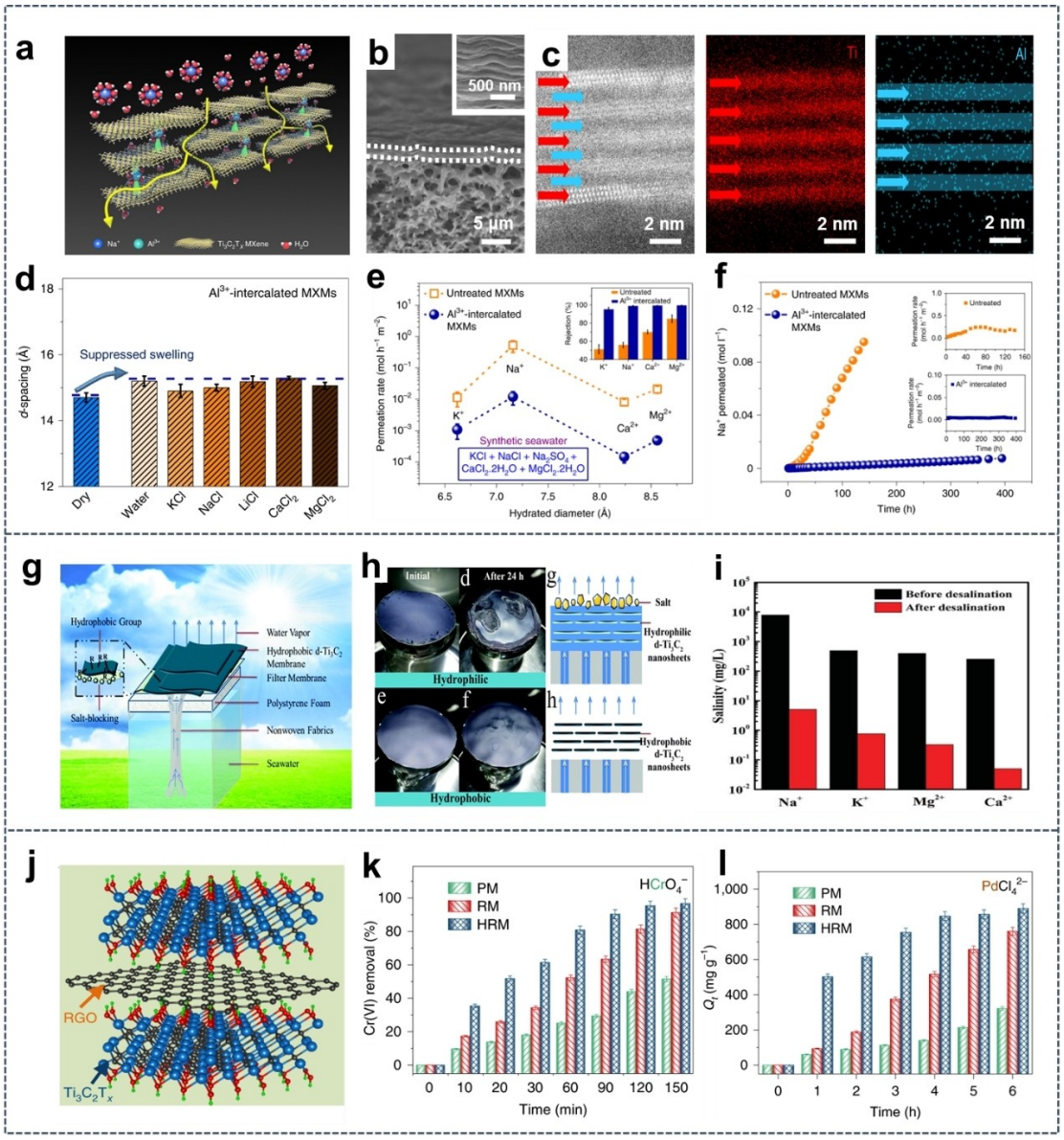

Figure 8. MXene membranes for salt and heavy metal ions removal. **(a)** Illustration of the Al^{3+}-intercalated MXene membrane for desalination. **(b)** Cross-sectional SEM and **(c)** HAADF images of the Al^{3+}-intercalated MXene membrane and corresponding element mapping. **(d)** *d*-Spacing of the Al^{3+}-intercalated MXene membrane in various salt solutions. **(e)** Corresponding desalination performance, and **(f)** Long-term stability test of the membrane. Reproduced with permission.[21a] Copyright 2020, Nature Publishing Group. **(g)** Hydrophobic MXene membrane based solar desalination device. **(h)** Comparisons of hydrophilic and hydrophobic MXene membranes after 24 h solar desalination. **(i)** Measured salinity of Na^+, K^+, Mg^{2+}, and Ca^{2+} before and after solar desalination. Reproduced with permission.[23g] Copyright 2018, Royal Society of Chemistry. **(j)** Schematic illustration of the $Ti_3C_2T_x$-rGO film. Comparisons of **(k)** $HCrO_4^-$ removal and **(l)** $PdCl_4^{2-}$ removal. Reproduced with permission.[79] Copyright 2019, Nature Publishing Group.

lished in this field, solving many underlying problems such as salt blocking, stability, low efficiency, and low evaporation rate.[23g,50,82] For example, Zhao et al.[23g] modified MXene nanosheets with PFDTMS and transferred the MXene membrane from hydrophilic into a hydrophobic state for solar-driven distillation, as illustrated in Figure 8g. The hydrophobic MXene membrane prevented the deposition and accumulation of salt on the membrane surface after 24 h desalination (Figure 8h). Accordingly, the hydrophobic MXene membrane exhibits excellent desalination performance. The rejection rates of Na^+, K^+, Mg^{2+}, and Ca^{2+} are all over 99.5 % (Figure 8i), demonstrating the capability of the MXene membrane in practical desalination.[23g]

The toxic heavy metal ions in wastewater are another major problem since they can be extremely harmful to human health and the whole ecosystem. However, the heavy metal ions always demonstrate extremely slow transport through MXene membranes. Generally, the heavy metal ions usually feature abundant charges (such as Pb^{2+}, Ba^{2+}, Ag^+), which directly leads to the strong interaction with the

negative charged surface groups of MXene and impedes their transport. Therefore, the removal of heavy metal ions mainly relies on the adsorption of MXene according to previous reports. However, the efficient removal of the anionic heavy metal ions such as $HCrO_4^-$, $AuCl_4^-$, and $PdCl_4^{2-}$ is impeded due to their large size and the negative charge. To improve the removal efficiency of these anionic heavy metal ions, Xie et al.[79] proposed a mitigating strategy to expand the interlayer spacing of the MXene film introducing reduced graphene oxide (rGO) as a spacer to mitigate the restacking of MXene nanosheets (Figure 8j). The introduction of the positively charged rGO greatly improved the efficiency of $HCrO_4^-$ removal and 91.3 % of $HCrO_4^-$ was removed after 150 min (Figure 8k). The adsorptive removal capacities of Pd^{2+} reach 890 mg g^{-1}, which is much higher than the comparisons (Figure 8l) and indicates the huge potential of MXene in adsorptive wastewater treatment.[79]

5. Challenges and prospects

In summary, the rapid growth of 2D materials has boosted the development of high-performance 2D materials-based membranes. The atomic thickness and the excellent processibility of the 2D nanosheets endow the corresponding 2D membranes with great potential to break the permeability-selectivity trade-off. In the concert of 2D membrane materials, the emergence of MXene nanosheets brings new opportunities for membrane technology.[83] Although the past years have seen the thriving development of MXene membranes in water purification, several challenging issues still need to be solved.

1. So far, only two kinds of MXene nanosheets have been applied for membrane preparation, $Ti_3C_2T_x$ and Ti_2CT_x, and over 99 % of the research on MXene membranes is based on $Ti_3C_2T_x$. However, over 30 kinds of MXenes have been successfully synthesized, featuring different physicochemical properties. Significantly, different MXenes relate to different surface functionalities and the corresponding membranes will be endowed with varying *d*-spacing thus targeting different separation processes. Exploring other kinds of MXenes is very important for further developing MXene membranes toward high-performance separation.
2. The etching method dominates the synthesis of MXene nanosheets. The toxic etchants are always the underlying risks in the synthesis process and the afterward application for water purification. Choosing a milder and non-toxic method to prepare nanosheets would greatly support the development of MXene membranes in drinking water production.
3. The preparation of porous MXene nanosheets is necessary. Since MXene nanosheets show no in-plane porosity, transport is governed through the *d*-spacing in the stack. However, the formation of uniform in-plane pores in the seven-atom layered $Ti_3C_2T_x$ is far more challenging than for single-atom graphene layers. How to develop porous MXene membranes and scale them up is a very tough but necessary task waiting to be solved.
4. Scalability of MXene membranes restricts their further development in large-scale water purification. The present preparation of membranes mainly relies on vacuum-assisted filtration for lamellar membranes or the casting method for Mixed Matrix Membranes (MMMs). However, it is very difficult to achieve continuous production and maintain the uniformity and quality of the membranes while scaling up. For MMMs, hollow fiber spinning seems attractive.
5. The separation mechanisms of MXene membranes require a more profound understanding of mass transport in the *d*-spacing between the nanosheets to support the design of 2D membranes. For example, how does the microenvironment of the nanochannels, such as the charges, the channel size, and the tortuosity, affect the transport of water molecules? From the theoretical and experimental perspectives, unraveling molecular water transport inside the MXene nanochannels remains challenging.
6. Besides the challenges mentioned above, the stability and compatibility of MXene membranes in practical separations should be considered. Moreover, expanding the application field of MXene membranes is quite important, such as purifying nuclear wastewater, extracting lithium from brine, and separating isotopes in aqueous solutions. Further, the removal of macromolecular organics from water near the polluters requires tailored membrane solutions: pharmaceuticals from waste water of hospitals, pesticides from agricultural outflows, dyes from industrial effluents, purification of landfill leachate, and removal of hormones.

The prosperous development of MXene membranes not only indicates the enormous potential of MXene but also demonstrates the underlying problems to some extent. However, both indicate an increased interest in pushing the boundaries of fundamental understanding and experimental studies of MXenes.

6. Abbreviations

2D	Two-dimensional
GO	graphene oxide
TMDs	metal dichalcogenides
MOFs	metal–organic frameworks
COFs	covalent-organic frameworks
HF	Hydrofluoric
VAF	vacuum-assisted filtration
LC	liquid-crystalline
PFDTMS	trimethoxy(perfluorodecyl)silane
ANF	Aramid nanofibers
MMMs	Mixed Matrix Membranes
AFM	Atomic Force Microscopy
E. coli	Escherichia coli
B. subtilis	Bacillus subtilis
EMI	electromagnetic interference

CNTs	carbon nanotubes
PVDF	Poly(vinylidene fluoride)
PES	Poly(ether sulfones)
AAO	Anodic Aluminum Oxide
PSS	poly(sodium 4-styrene sulfonate)
PVA	poly(vinyl alcohol)
PEI	polyethyleneimine
PAN	polyacrylonitrile
PSF	polysulfone
PA	polyamide
MB	methylene blue
PDDA	poly(diallyldimethylammonium chloride)
NPs	nanoparticles
PEN	poly(arylene ether nitrile
HCl	hydrochloric acid
BSA	bovine serum albumin
Cyt. C	Cytochrome
EB	Evans blue
RhB	rhodamine B
SEM	Scanning Electron Microscopy
HAADF	high-angle annular dark-field
rGO	reduced graphene oxide

Acknowledgements

We gratefully acknowledge the funding from the Nation Natural Science Foundation of China (22138005, 22141001, 22378226), Young Elite Scientists Sponsorship Program by BAST. Open Access funding enabled and organized by Projekt DEAL.

Conflict of Interest

The authors declare no conflict of interest.

Data Availability Statement

The data that support the findings of this study are available from the corresponding author upon reasonable request.

Keywords: 2D Membrane · MXene · Nanosheets · Water Purification

[1] a) M. M. Mekonnen, A. Y. Hoekstra, *Sci. Adv.* **2016**, *2*, e1500323; b) T. Tao, K. Xin, *Nature* **2014**, *511*, 527–528.
[2] a) M. A. Shannon, P. W. Bohn, M. Elimelech, J. G. Georgiadis, B. J. Mariñas, A. M. Mayes, *Nature* **2008**, *452*, 301–310; b) M. Elimelech, W. A. Phillip, *Science* **2011**, *333*, 712–717; c) Y. Xu, Z. Mao, R. Qu, J. Wang, J. Yu, X. Luo, M. Shi, X. Mao, J. Ding, B. Liu, *Nat. Water* **2023**, *1*, 95–103; d) D. S. Sholl, R. P. Lively, *Nature* **2016**, *532*, 435–437.
[3] G. Ni, G. Li, S. V. Boriskina, H. Li, W. Yang, T. Zhang, G. Chen, *Nat. Energy* **2016**, *1*, 16126.
[4] a) F. Fu, Q. Wang, *J. Environ. Manage.* **2011**, *92*, 407–418; b) R. P. Schwarzenbach, B. I. Escher, K. Fenner, T. B. Hofstetter, C. A. Johnson, U. von Gunten, B. Wehrli, *Science* **2006**, *313*, 1072–1077.
[5] a) M. R. Chowdhury, J. Steffes, B. D. Huey, J. R. McCutcheon, *Science* **2018**, *361*, 682–686; b) X. You, H. Wu, R. Zhang, Y. Su, L. Cao, Q. Yu, J. Yuan, K. Xiao, M. He, Z. Jiang, *Nat. Commun.* **2019**, *10*, 4160; c) Z. Jiang, S. Karan, A. G. Livingston, *Adv. Mater.* **2018**, *30*, 1705973; d) X. Wang, Z. Lin, J. Gao, Z. Xu, X. Li, N. Xu, J. Li, Y. Song, H. Fu, W. Zhao, S. Wang, B. Zhu, R. Wang, J. Zhu, *Nat. Water* **2023**, *1*, 391–398; e) D. Cohen-Tanugi, R. K. McGovern, S. H. Dave, J. H. Lienhard, J. C. Grossman, *Energy Environ. Sci.* **2014**, *7*, 1134–1141; f) S. P. Nunes, P. Z. Culfaz-Emecen, G. Z. Ramon, T. Visser, G. H. Koops, W. Jin, M. Ulbricht, *J. Membr. Sci.* **2020**, *598*, 117761.
[6] a) R. R. Nair, H. A. Wu, P. N. Jayaram, I. V. Grigorieva, A. K. Geim, *Science* **2012**, *335*, 442–444; b) R. K. Joshi, P. Carbone, F. C. Wang, V. G. Kravets, Y. Su, I. V. Grigorieva, H. A. Wu, A. K. Geim, R. R. Nair, *Science* **2014**, *343*, 752–754; c) B. Mi, *Science* **2014**, *343*, 740–742; d) M. Heiranian, A. B. Farimani, N. R. Aluru, *Nat. Commun.* **2015**, *6*, 8616.
[7] a) G. Liu, W. Jin, N. Xu, *Chem. Soc. Rev.* **2015**, *44*, 5016–5030; b) A. K. Geim, K. S. Novoselov, *Nat. Mater.* **2007**, *6*, 183–191; c) H. W. Kim, H. W. Yoon, S.-M. Yoon, B. M. Yoo, B. K. Ahn, Y. H. Cho, H. J. Shin, H. Yang, U. Paik, S. Kwon, J.-Y. Choi, H. B. Park, *Science* **2013**, *342*, 91–95; d) J. C. Meyer, A. K. Geim, M. I. Katsnelson, K. S. Novoselov, T. J. Booth, S. Roth, *Nature* **2007**, *446*, 60–63; e) H. Wang, Y. Wei, L. Ding, in *MXene Membranes for Separations*, Wiley-VCH, Weinheim, **2022**, pp. 9–24.
[8] M. Naguib, M. Kurtoglu, V. Presser, J. Lu, J. Niu, M. Heon, L. Hultman, Y. Gogotsi, M. W. Barsoum, *Adv. Mater.* **2011**, *23*, 4248–4253.
[9] a) M. Naguib, V. N. Mochalin, M. W. Barsoum, Y. Gogotsi, *Adv. Mater.* **2014**, *26*, 992–1005; b) O. Mashtalir, M. Naguib, V. N. Mochalin, Y. Dall'Agnese, M. Heon, M. W. Barsoum, Y. Gogotsi, *Nat. Commun.* **2013**, *4*, 1716.
[10] a) M. Alhabeb, K. Maleski, B. Anasori, P. Lelyukh, L. Clark, S. Sin, Y. Gogotsi, *Chem. Mater.* **2017**, *29*, 7633–7644; b) M. Ghidiu, M. R. Lukatskaya, M.-Q. Zhao, Y. Gogotsi, M. W. Barsoum, *Nature* **2014**, *516*, 78–81; c) M. R. Lukatskaya, O. Mashtalir, C. E. Ren, Y. Dall'Agnese, P. Rozier, P. L. Taberna, M. Naguib, P. Simon, M. W. Barsoum, Y. Gogotsi, *Science* **2013**, *341*, 1502–1505.
[11] D. Xiong, X. Li, Z. Bai, S. Lu, *Small* **2018**, *14*, 1703419.
[12] a) A. Lipatov, M. Alhabeb, H. Lu, S. Zhao, M. J. Loes, N. S. Vorobeva, Y. Dall′Agnese, Y. Gao, A. Gruverman, Y. Gogotsi, A. Sinitskii, *Adv. Electron. Mater.* **2020**, *6*, 1901382; b) A. Lipatov, H. Lu, M. Alhabeb, B. Anasori, A. Gruverman, Y. Gogotsi, A. Sinitskii, *Sci. Adv.* **2018**, *4*, eaat0491.
[13] A. VahidMohammadi, J. Rosen, Y. Gogotsi, *Science* **2021**, *372*, eabf1581.
[14] a) X. Wang, S. Kajiyama, H. Iinuma, E. Hosono, S. Oro, I. Moriguchi, M. Okubo, A. Yamada, *Nat. Commun.* **2015**, *6*, 6544; b) J. Pang, R. G. Mendes, A. Bachmatiuk, L. Zhao, H. Q. Ta, T. Gemming, H. Liu, Z. Liu, M. H. Rummeli, *Chem. Soc. Rev.* **2019**, *48*, 72–133.
[15] a) M.-S. Cao, Y.-Z. Cai, P. He, J.-C. Shu, W.-Q. Cao, J. Yuan, *Chem. Eng. J.* **2019**, *359*, 1265–1302; b) M. Han, C. E. Shuck, R. Rakhmanov, D. Parchment, B. Anasori, C. M. Koo, G. Friedman, Y. Gogotsi, *ACS Nano* **2020**, *14*, 5008–5016; c) A. Iqbal, F. Shahzad, K. Hantanasirisakul, M.-K. Kim, J. Kwon, J. Hong, H. Kim, D. Kim, Y. Gogotsi, C. M. Koo, *Science* **2020**, *369*, 446–450; d) T. Yun, H. Kim, A. Iqbal, Y. S. Cho, G. S. Lee, M.-K. Kim, S. J. Kim, D. Kim, Y. Gogotsi, S. O. Kim, C. M. Koo, *Adv. Mater.* **2020**, *32*, 1906769.
[16] a) Y. Ma, N. Liu, L. Li, X. Hu, Z. Zou, J. Wang, S. Luo, Y. Gao, *Nat. Commun.* **2017**, *8*, 1207; b) S. J. Kim, H.-J. Koh,

C. E. Ren, O. Kwon, K. Maleski, S.-Y. Cho, B. Anasori, C.-K. Kim, Y.-K. Choi, J. Kim, Y. Gogotsi, H.-T. Jung, *ACS Nano* **2018**, *12*, 986–993; c) Y.-Z. Zhang, K. H. Lee, D. H. Anjum, R. Sougrat, Q. Jiang, H. Kim, H. N. Alshareef, *Sci. Adv.* **2018**, *4*, eaat0098.

[17] a) L. Ding, Y. Wei, Y. Wang, H. Chen, J. Caro, H. Wang, *Angew. Chem. Int. Ed.* **2017**, *56*, 1825–1829; b) M. Yi, M. Wang, Y. Wang, Y. Wang, J. Chang, A. K. Kheirabad, H. He, J. Yuan, M. Zhang, *Angew. Chem. Int. Ed.* **2022**, *61*, e202202515; c) L. Ding, M. Zheng, D. Xiao, Z. Zhao, J. Xue, S. Zhang, J. Caro, H. Wang, *Angew. Chem. Int. Ed.* **2022**, *61*, e202206152; d) G. Liu, W. Jin, N. Xu, *Angew. Chem. Int. Ed.* **2016**, *55*, 13384–13397.

[18] Q. Peng, J. Guo, Q. Zhang, J. Xiang, B. Liu, A. Zhou, R. Liu, Y. Tian, *J. Am. Chem. Soc.* **2014**, *136*, 4113–4116.

[19] a) Z. Lu, Y. Wu, L. Ding, Y. Wei, H. Wang, *Angew. Chem. Int. Ed.* **2021**, *60*, 22265–22269; b) C. E. Ren, K. B. Hatzell, M. Alhabeb, Z. Ling, K. A. Mahmoud, Y. Gogotsi, *J. Phys. Chem. Lett.* **2015**, *6*, 4026–4031.

[20] a) L. Ding, Y. Wei, L. Li, T. Zhang, H. Wang, J. Xue, L.-X. Ding, S. Wang, J. Caro, Y. Gogotsi, *Nat. Commun.* **2018**, *9*, 155; b) J. Shen, G. Liu, Y. Ji, Q. Liu, L. Cheng, K. Guan, M. Zhang, G. Liu, J. Xiong, J. Yang, W. Jin, *Adv. Funct. Mater.* **2018**, *28*, 1801511.

[21] a) L. Ding, L. Li, Y. Liu, Y. Wu, Z. Lu, J. Deng, Y. Wei, J. Caro, H. Wang, *Nat. Sustainability* **2020**, *3*, 296–302; b) J. Wang, Z. Zhang, J. Zhu, M. Tian, S. Zheng, F. Wang, X. Wang, L. Wang, *Nat. Commun.* **2020**, *11*, 3540.

[22] X. Wu, X. Cui, W. Wu, J. Wang, Y. Li, Z. Jiang, *Angew. Chem. Int. Ed.* **2019**, *58*, 18524–18529.

[23] a) X. Wu, L. Hao, J. Zhang, X. Zhang, J. Wang, J. Liu, *J. Membr. Sci.* **2016**, *515*, 175–188; b) K. M. Kang, D. W. Kim, C. E. Ren, K. M. Cho, S. J. Kim, J. H. Choi, Y. T. Nam, Y. Gogotsi, H.-T. Jung, *ACS Appl. Mater. Interfaces* **2017**, *9*, 44687–44694; c) R. Li, L. Zhang, L. Shi, P. Wang, *ACS Nano* **2017**, *11*, 3752–3759; d) J. Lao, R. Lv, J. Gao, A. Wang, J. Wu, J. Luo, *ACS Nano* **2018**, *12*, 12464–12471; e) R. P. Pandey, K. Rasool, V. E. Madhavan, B. Aïssa, Y. Gogotsi, K. A. Mahmoud, *J. Mater. Chem. A* **2018**, *6*, 3522–3533; f) C. E. Ren, M. Alhabeb, B. W. Byles, M.-Q. Zhao, B. Anasori, E. Pomerantseva, K. A. Mahmoud, Y. Gogotsi, *ACS Appl. Nano Mater.* **2018**, *1*, 3644–3652; g) J. Zhao, Y. Yang, C. Yang, Y. Tian, Y. Han, J. Liu, X. Yin, W. Que, *J. Mater. Chem. A* **2018**, *6*, 16196–16204; h) X. Gao, Z.-K. Li, J. Xue, Y. Qian, L.-Z. Zhang, J. Caro, H. Wang, *J. Membr. Sci.* **2019**, *586*, 162–169; i) Z.-K. Li, Y. Liu, L. Li, Y. Wei, J. Caro, H. Wang, *J. Membr. Sci.* **2019**, *592*, 117361; j) Y. Wu, L. Ding, Z. Lu, J. Deng, Y. Wei, *J. Membr. Sci.* **2019**, *590*, 117300; k) Z. Zhang, S. Yang, P. Zhang, J. Zhang, G. Chen, X. Feng, *Nat. Commun.* **2019**, *10*, 2920; l) L. Ding, D. Xiao, Z. Lu, J. Deng, Y. Wei, J. Caro, H. Wang, *Angew. Chem. Int. Ed.* **2020**, *59*, 8720–8726; m) Z.-K. Li, Y. Wei, X. Gao, L. Ding, Z. Lu, J. Deng, X. Yang, J. Caro, H. Wang, *Angew. Chem. Int. Ed.* **2020**, *59*, 9751–9756; n) J. Deng, Z. Lu, L. Ding, Z.-K. Li, Y. Wei, J. Caro, H. Wang, *Chem. Eng. J.* **2021**, *408*, 127806.

[24] a) Q. Tang, Z. Zhou, P. Shen, *J. Am. Chem. Soc.* **2012**, *134*, 16909–16916; b) M. R. Lukatskaya, S. Kota, Z. Lin, M.-Q. Zhao, N. Shpigel, M. D. Levi, J. Halim, P.-L. Taberna, M. W. Barsoum, P. Simon, Y. Gogotsi, *Nat. Energy* **2017**, *2*, 17105; c) H. Wang, Y. Wei, L. Ding, in *MXene Membranes for Separations*, Wiley-VCH, Weinheim, **2022**, pp. 1–8.

[25] G. P. Lim, C. F. Soon, A. A. Al-Gheethi, M. Morsin, K. S. Tee, *Ceram. Int.* **2022**, *48*, 16477–16491.

[26] M. Naguib, O. Mashtalir, J. Carle, V. Presser, J. Lu, L. Hultman, Y. Gogotsi, M. W. Barsoum, *ACS Nano* **2012**, *6*, 1322–1331.

[27] L. Verger, C. Xu, V. Natu, H.-M. Cheng, W. Ren, M. W. Barsoum, *Curr. Opin. Solid State Mater. Sci.* **2019**, *23*, 149–163.

[28] M. Shen, W. Jiang, K. Liang, S. Zhao, R. Tang, L. Zhang, J.-Q. Wang, *Angew. Chem. Int. Ed.* **2021**, *60*, 27013–27018.

[29] T. Li, L. Yao, Q. Liu, J. Gu, R. Luo, J. Li, X. Yan, W. Wang, P. Liu, B. Chen, W. Zhang, W. Abbas, R. Naz, D. Zhang, *Angew. Chem. Int. Ed.* **2018**, *57*, 6115–6119.

[30] W. Sun, S. A. Shah, Y. Chen, Z. Tan, H. Gao, T. Habib, M. Radovic, M. J. Green, *J. Mater. Chem. A* **2017**, *5*, 21663–21668.

[31] D. Wang, C. Zhou, A. S. Filatov, W. Cho, F. Lagunas, M. Wang, S. Vaikuntanathan, C. Liu, R. F. Klie, D. V. Talapin, *Science* **2023**, *379*, 1242–1247.

[32] Z. Zhang, F. Zhang, H. Wang, C. H. Chan, W. Lu, J.-y. Dai, *J. Mater. Chem. C* **2017**, *5*, 10822–10827.

[33] X. Xiao, H. Yu, H. Jin, M. Wu, Y. Fang, J. Sun, Z. Hu, T. Li, J. Wu, L. Huang, Y. Gogotsi, J. Zhou, *ACS Nano* **2017**, *11*, 2180–2186.

[34] G. Liu, J. Shen, Y. Ji, Q. Liu, G. Liu, J. Yang, W. Jin, *J. Mater. Chem. A* **2019**, *7*, 12095–12104.

[35] a) Y. Zhao, Q. Yu, W.-W. Cheng, J.-Q. Li, A.-Q. Zhang, X. Lei, Y. Yang, S.-Y. Qin, *ACS Nano* **2022**, *16*, 5454–5462; b) J. Zhang, S. Uzun, S. Seyedin, P. A. Lynch, B. Akuzum, Z. Wang, S. Qin, M. Alhabeb, C. E. Shuck, W. Lei, E. C. Kumbur, W. Yang, X. Wang, G. Dion, J. M. Razal, Y. Gogotsi, *ACS Cent. Sci.* **2020**, *6*, 254–265; c) J. Zhang, N. Kong, S. Uzun, A. Levitt, S. Seyedin, P. A. Lynch, S. Qin, M. Han, W. Yang, J. Liu, X. Wang, Y. Gogotsi, J. M. Razal, *Adv. Mater.* **2020**, *32*, 2001093.

[36] A. Akbari, P. Sheath, S. T. Martin, D. B. Shinde, M. Shaibani, P. C. Banerjee, R. Tkacz, D. Bhattacharyya, M. Majumder, *Nat. Commun.* **2016**, *7*, 10891.

[37] S. Wan, X. Li, Y. Wang, Y. Chen, X. Xie, R. Yang, A. P. Tomsia, L. Jiang, Q. Cheng, *Proc. Natl. Acad. Sci. USA* **2020**, *117*, 27154–27161.

[38] a) R. Zhang, Y. Liu, M. He, Y. Su, X. Zhao, M. Elimelech, Z. Jiang, *Chem. Soc. Rev.* **2016**, *45*, 5888–5924; b) N. Savage, M. S. Diallo, *J. Nanopart. Res.* **2005**, *7*, 331–342.

[39] K. Rasool, M. Helal, A. Ali, C. E. Ren, Y. Gogotsi, K. A. Mahmoud, *ACS Nano* **2016**, *10*, 3674–3684.

[40] H. Yu, X. Xu, Z. Xie, X. Huang, L. Lin, Y. Jiao, H. Li, *ACS Appl. Mater. Interfaces* **2022**, *14*, 36947–36956.

[41] a) J. Saththasivam, K. Wang, W. Yiming, Z. Liu, K. A. Mahmoud, *RSC Adv.* **2019**, *9*, 16296–16304; b) H. Zhang, Z. Wang, Y. Shen, P. Mu, Q. Wang, J. Li, *J. Colloid Interface Sci.* **2020**, *561*, 861–869.

[42] A. Alkhudhiri, N. Darwish, N. Hilal, *Desalination* **2012**, *287*, 2–18.

[43] a) P. Tao, G. Ni, C. Song, W. Shang, J. Wu, J. Zhu, G. Chen, T. Deng, *Nat. Energy* **2018**, *3*, 1031–1041; b) L. Zhu, M. Gao, C. K. N. Peh, G. W. Ho, *Nano Energy* **2019**, *57*, 507–518.

[44] F. Shahzad, M. Alhabeb, C. B. Hatter, B. Anasori, S. Man Hong, C. M. Koo, Y. Gogotsi, *Science* **2016**, *353*, 1137–1140.

[45] a) Y. Liu, J. Zhang, X. Zhang, Y. Li, J. Wang, *ACS Appl. Mater. Interfaces* **2016**, *8*, 20352–20363; b) N. Li, T.-J. Lou, W. Wang, M. Li, L.-C. Jing, Z.-X. Yang, R.-Y. Chang, J. Li, H.-Z. Geng, *J. Membr. Sci.* **2023**, *668*, 121271.

[46] a) H. Zhang, X. Shen, E. Kim, M. Wang, J.-H. Lee, H. Chen, G. Zhang, J.-K. Kim, *Adv. Funct. Mater.* **2022**, *32*, 2111794; b) Z. Yu, P. Wu, *Adv. Mater. Technol.* **2020**, *5*, 2000065.

[47] Y. Zhang, D. Chen, N. Li, Q. Xu, H. Li, J. He, J. Lu, *ACS Appl. Mater. Interfaces* **2022**, *14*, 10237–10245.

[48] a) Y. Cai, L. Zhang, R. Fang, Y. Wang, J. Wang, *Sep. Purif. Technol.* **2022**, *292*, 121019; b) H. Xu, J. Ma, M. Ding, Z. Xie, *Desalination* **2022**, *529*, 115643; c) H. Zhang, Y. Zheng, H. Zhou, S. Zhu, J. Yang, *Sep. Purif. Technol.* **2023**, *305*, 122425.

[49] L. Hao, H. Zhang, X. Wu, J. Zhang, J. Wang, Y. Li, *Composites Part A* **2017**, *100*, 139–149.
[50] B. Zhang, P. W. Wong, J. Guo, Y. Zhou, Y. Wang, J. Sun, M. Jiang, Z. Wang, A. K. An, *Nat. Commun.* **2022**, *13*, 3315.
[51] R. Tkacz, R. Oldenbourg, A. Fulcher, M. Miansari, M. Majumder, *J. Phys. Chem. C* **2014**, *118*, 259–267.
[52] X. Wang, Q. Li, J. Zhang, H. Huang, S. Wu, Y. Yang, *J. Membr. Sci.* **2020**, *603*, 118036.
[53] D. Qadir, H. Mukhtar, L. K. Keong, *Sep. Purif. Rev.* **2017**, *46*, 62–80.
[54] Q. Li, T. Zhang, Z. Dai, F. Su, X. Xia, P. Dong, J. Zhang, *J. Membr. Sci.* **2023**, *671*, 121385.
[55] M.-Q. Zhao, N. Trainor, C. E. Ren, M. Torelli, B. Anasori, Y. Gogotsi, *Adv. Mater. Technol.* **2019**, *4*, 1800639.
[56] Y.-y. Yao, T. Wang, L.-g. Wu, H.-l. Chen, *Desalination* **2022**, *543*, 116116.
[57] X. Zhu, X. Zhang, J. Li, X. Luo, D. Xu, D. Wu, W. Wang, X. Cheng, G. Li, H. Liang, *J. Membr. Sci.* **2021**, *635*, 119536.
[58] T. F. Ajibade, H. Tian, K. Hassan Lasisi, Q. Xue, W. Yao, K. Zhang, *Sep. Purif. Technol.* **2021**, *275*, 119135.
[59] a) J. Jang, Y. Kang, K. Jang, S. Kim, S.-S. Chee, I. S. Kim, *Chem. Eng. J.* **2022**, *437*, 135297; b) J. Li, L. Li, Y. Xu, J. Zhu, F. Liu, J. Shen, Z. Wang, J. Lin, *Chem. Eng. J.* **2022**, *427*, 132070; c) Y. Sun, F. Yi, R.-H. Li, X. Min, H. Qin, S.-Q. Cheng, Y. Liu, *Angew. Chem. Int. Ed.* **2022**, *61*, e202200482.
[60] a) H. E. Karahan, K. Goh, C. Zhang, E. Yang, C. Yıldırım, C. Y. Chuah, M. G. Ahunbay, J. Lee, Ş. B. Tantekin-Ersolmaz, Y. Chen, T.-H. Bae, *Adv. Mater.* **2020**, *32*, 1906697; b) A. Khosla, Sonu, H. T. A. Awan, K. Singh, Gaurav, R. Walvekar, Z. Zhao, A. Kaushik, M. Khalid, V. Chaudhary, *Adv. Sci.* **2022**, *9*, 2203527.
[61] R. P. Pandey, P. A. Rasheed, T. Gomez, R. S. Azam, K. A. Mahmoud, *J. Membr. Sci.* **2020**, *607*, 118139.
[62] a) I. Raheem, N. M. Mubarak, R. R. Karri, N. H. Solangi, A. S. Jatoi, S. A. Mazari, M. Khalid, Y. H. Tan, J. R. Koduru, G. Malafaia, *Chemosphere* **2023**, *311*, 137056; b) N. H. Solangi, N. M. Mubarak, R. R. Karri, S. A. Mazari, S. K. Kailasa, A. Alfantazi, *Chemosphere* **2023**, *314*, 137643; c) L. Huang, L. Ding, H. Wang, *Small Sci.* **2021**, *1*, 2100013.
[63] Z. Ling, C. E. Ren, M.-Q. Zhao, J. Yang, J. M. Giammarco, J. Qiu, M. W. Barsoum, Y. Gogotsi, *Proc. Natl. Acad. Sci. USA* **2014**, *111*, 16676–16681.
[64] S. Hong, F. Ming, Y. Shi, R. Li, I. S. Kim, C. Y. Tang, H. N. Alshareef, P. Wang, *ACS Nano* **2019**, *13*, 8917–8925.
[65] C. Wang, R. Cheng, P.-X. Hou, Y. Ma, A. Majeed, X. Wang, C. Liu, *ACS Appl. Mater. Interfaces* **2020**, *12*, 43032–43041.
[66] a) L. Xu, Y. Chen, W. Su, J. Cui, S. Wei, *Sep. Purif. Technol.* **2023**, *309*, 123024; b) Y. Fan, J. Li, S. Wang, X. Meng, W. Zhang, Y. Jin, N. Yang, X. Tan, J. Li, S. Liu, *Chem. Eng. J.* **2020**, *401*, 126073; c) S. Li, L. Wang, J. Peng, M. Zhai, W. Shi, *Chem. Eng. J.* **2019**, *366*, 192–199; d) L. Wang, H. Song, L. Yuan, Z. Li, P. Zhang, J. K. Gibson, L. Zheng, H. Wang, Z. Chai, W. Shi, *Environ. Sci. Technol.* **2019**, *53*, 3739–3747; e) B.-M. Jun, N. Her, C. M. Park, Y. Yoon, *Environ. Sci. Water Res. Technol.* **2020**, *6*, 173–180; f) B.-M. Jun, C. M. Park, J. Heo, Y. Yoon, *J. Environ. Manage.* **2020**, *256*, 109940.
[67] a) L. Gao, C. Li, W. Huang, S. Mei, H. Lin, Q. Ou, Y. Zhang, J. Guo, F. Zhang, S. Xu, H. Zhang, *Chem. Mater.* **2020**, *32*, 1703–1747; b) R. S. Azam, D. A. Almasri, R. Alfahel, A. H. Hawari, M. K. Hassan, A. A. Elzatahry, K. A. Mahmoud, *Membranes* **2022**, *12*, 406.
[68] J. Caro, *Chem. Ing. Tech.* **2018**, *90*, 1759–1768.
[69] G. Yang, Z. Xie, A. W. Thornton, C. M. Doherty, M. Ding, H. Xu, M. Cran, D. Ng, S. Gray, *J. Membr. Sci.* **2020**, *614*, 118490.
[70] Q. Feng, Y. Zhan, W. Yang, H. Dong, A. Sun, L. Li, X. Chen, Y. Chen, *Sep. Purif. Technol.* **2022**, *298*, 121635.
[71] K. Rajavel, S. Shen, T. Ke, D. Lin, *2D Mater.* **2019**, *6*, 035040.
[72] M. Lakemeyer, W. Zhao, F. A. Mandl, P. Hammann, S. A. Sieber, *Angew. Chem. Int. Ed.* **2018**, *57*, 14440–14475.
[73] a) Y. Li, R. Dai, H. Zhou, X. Li, Z. Wang, *ACS Appl. Nano Mater.* **2021**, *4*, 6328–6336; b) T. Yousaf, A. Areeb, M. Murtaza, A. Munir, Y. Khan, A. Waseem, *ACS Omega* **2022**, *7*, 19502–19512; c) S. Zhang, S. Liao, F. Qi, R. Liu, T. Xiao, J. Hu, K. Li, R. Wang, Y. Min, *J. Hazard. Mater.* **2020**, *384*, 121367; d) F. Liao, Z. Xu, Z. Fan, Q. Meng, B. Lv, X. Ye, C. Shen, G. Zhang, *J. Mater. Chem. A* **2021**, *9*, 12236–12243; e) Z. Huang, Q. Zeng, Y. Liu, Y. Xu, R. Li, H. Hong, L. Shen, H. Lin, *J. Membr. Sci.* **2021**, *640*, 119854.
[74] C. Feng, K. Ou, Z. Zhang, Y. Liu, Y. Huang, Z. Wang, Y. Lv, Y.-E. Miao, Y. Wang, Q. Lan, T. Liu, *J. Membr. Sci.* **2022**, *658*, 120761.
[75] G. Zeng, Z. He, T. Wan, T. Wang, Z. Yang, Y. Liu, Q. Lin, Y. Wang, A. Sengupta, S. Pu, *Sep. Purif. Technol.* **2022**, *292*, 121037.
[76] a) H. Wang, Y. Zhai, Y. Li, Y. Cao, B. Shi, R. Li, Z. Zhu, H. Jiang, Z. Guo, M. Wang, L. Chen, Y. Liu, K.-G. Zhou, F. Pan, Z. Jiang, *Nat. Commun.* **2022**, *13*, 7123; b) J. Lu, H. Zhang, J. Hou, X. Li, X. Hu, Y. Hu, C. D. Easton, Q. Li, C. Sun, A. W. Thornton, M. R. Hill, X. Zhang, G. Jiang, J. Z. Liu, A. J. Hill, B. D. Freeman, L. Jiang, H. Wang, *Nat. Mater.* **2020**, *19*, 767–774; c) H. Zhang, J. Hou, Y. Hu, P. Wang, R. Ou, L. Jiang, J. Z. Liu, B. D. Freeman, A. J. Hill, H. Wang, *Sci. Adv.* **2018**, *4*, eaaq0066.
[77] a) M. Ding, H. Xu, W. Chen, G. Yang, Q. Kong, D. Ng, T. Lin, Z. Xie, *J. Membr. Sci.* **2020**, *600*, 117871; b) P. Ying, B. Ai, W. Hu, Y. Geng, L. Li, K. Sun, S. C. Tan, W. Zhang, M. Li, *Nano Energy* **2021**, *89*, 106443.
[78] I. Dzidic, P. Kebarle, *J. Phys. Chem.* **1970**, *74*, 1466–1474.
[79] X. Xie, C. Chen, N. Zhang, Z.-R. Tang, J. Jiang, Y.-J. Xu, *Nat. Sustainability* **2019**, *2*, 856–862.
[80] G. Liu, J. Shen, Q. Liu, G. Liu, J. Xiong, J. Yang, W. Jin, *J. Membr. Sci.* **2018**, *548*, 548–558.
[81] a) C. Charcosset, *Desalination* **2009**, *245*, 214–231; b) D. González, J. Amigo, F. Suárez, *Renew. Sustainable Energy Rev.* **2017**, *80*, 238–259.
[82] a) M. Mustakeem, J. K. El-Demellawi, M. Obaid, F. Ming, H. N. Alshareef, N. Ghaffour, *ACS Appl. Mater. Interfaces* **2022**, *14*, 5265–5274; b) B. Zhang, Q. Gu, C. Wang, Q. Gao, J. Guo, P. W. Wong, C. T. Liu, A. K. An, *ACS Appl. Mater. Interfaces* **2021**, *13*, 3762–3770.
[83] H. Wang, Y. Wei, L. Ding, in *MXene Membranes for Separations*, Wiley-VCH, Weinheim, **2022**, pp. 197–201.

Manuscript received: August 2, 2023
Accepted manuscript online: August 24, 2023
Version of record online: September 15, 2023